Application of Digital Twins for Testing Connectivity, Automation, and Cooperation Applications

Final Report

PROJECT NO.
BED29 TWO 977 - 12

Prepared for

Florida Department of Transportation

Prepared by

Florida International University

July 2026

Disclaimer

The opinions, findings, and conclusions expressed in this publication are those of the authors and not necessarily those of the State of Florida.

METRIC CONVERSION CHART

Approximate Conversions to SI* Units					**Approximate Conversions from SI Units**				
Symbol	When You Know	Multiply By	To Find	Symbol	Symbol	When You Know	Multiply By	To Find	Symbol
LENGTH					**LENGTH**				
in	inches	25.4	millimeters	mm	mm	millimeters	0.039	inches	in
ft	feet	0.305	meters	m	m	meters	3.28	feet	ft
yd	yards	0.914	meters	m	m	meters	1.09	yards	yd
mi	miles	1.61	kilometers	km	km	kilometers	0.621	miles	mi
AREA					**AREA**				
in^2	square inches	645.2	millimeters squared	mm^2	mm^2	millimeters squared	0.0016	square inches	in^2
ft^2	square feet	0.093	meters squared	m^2	m^2	meters squared	10.764	square feet	ft^2
yd^2	square yards	0.836	meters squared	m^2	m^2	meters squared	1.196	square yards	yd^2
ac	acres	0.405	hectares	ha	ha	hectares	2.47	acres	ac
mi^2	square miles	2.59	kilometers squared	km^2	km^2	kilometers squared	0.386	square miles	mi^2
VOLUME					**VOLUME**				
fl oz	fluid ounces	29.57	milliliters	ml	ml	milliliters	0.034	fluid ounces	fl oz
gal	gallons	3.785	liters	L	L	liters	0.264	gallons	gal
ft^3	cubic feet	0.028	meters cubed	m^3	m^3	meters cubed	35.315	cubic feet	ft^3
yd^3	cubic yards	0.765	meters cubed	m^3	m^3	meters cubed	1.308	cubic yards	yd^3
NOTE: Volumes greater than 1000 L shall be shown in m^3.									
MASS					**MASS**				
oz	ounces	28.35	grams	g	g	grams	0.035	ounces	oz
lb	pounds	0.454	kilograms	kg	kg	kilograms	2.205	pounds	lb
T	short tons (2000 lb)	0.907	megagrams	Mg	Mg	megagrams	1.102	short tons (2000 lb)	T
TEMPERATURE (exact)					**TEMPERATURE (exact)**				
°F	Fahrenheit	(F-32)/1.8	Celsius	°C	°C	Celsius	1.8C+32	Fahrenheit	°F
*SI is the symbol for the International System of Measurement									

TECHNICAL REPORT DOCUMENTATION PAGE

1. Report No.	2. Government Accession No.	3. Recipient's Catalog No.
4. Title and Subtitle Application of Digital Twins for Testing Connectivity, Automation, and Cooperation Applications		5. Report Date July 2026 6. Performing Organization Code
7. Author(s) Mohammed Hadi, Ph.D., PE, and Chonlachart Jeenprasom		8. Performing Organization Report No. 10. Work Unit No.
9. Performing Organization Name and Address Florida International University 10555 W Flagler St Miami, FL 33174		11. Contract or Grant No. BED29 TWO 977 - 12
12. Sponsoring Agency Name and Address Florida Department of Transportation 605 Suwannee Street, MS 30 Tallahassee, FL 32399		13. Type of Report and Period Covered Draft Final Report April 2025 to July 2026 14. Sponsoring Agency Code
15. Supplementary Notes The Project Managers from FDOT is Brett Wood, PSM		

16. Abstract

This study investigated the use of co-simulation for evaluating cooperative driving automation (CDA) applications within a work zone environment. The examined use case focused on the merging maneuvers of a single CDA-equipped vehicle into either a CDA platoon or a traffic stream consisting of human-driven vehicles near a work zone with a one-lane blockage. The findings demonstrate that co-simulation can serve as an effective component of automated vehicle and CDA testing, particularly in complex and challenging environments such as work zones. The study further demonstrated that cooperative lane-changing behavior near work zones can be systematically assessed within a controlled simulation environment, and that the resulting performance measures can help identify limitations and guide improvements to existing automated and cooperative driving algorithms and control logic.

17. Key Words Co-simulation, Digital Twin, Cooperative Driving Automation, Automated Vehicles, Testing		18. Distribution Statement No restrictions.	
19. Security Classif. (of this report) Unclassified	20. Security Classif. (of this page) Unclassified	21. No. of Pages 52	22. Price

Form DOT F 1700.7 (8-72) Reproduction of completed page authorized.

Executive Summary

Simulation and digital twin technologies continue to play a critical role in cooperative driving automation (CDA) research, testing, and evaluation. Work zones present particularly challenging environments for automated vehicles (AVs) because of lane closures, temporary traffic control configurations, and the complex interactions among human-driven vehicles, connected and automated vehicles (CAVs), and cooperative automated vehicle platoons. These conditions complicate lane-changing and merging maneuvers and may adversely affect both traffic operations and safety.

Co-simulation is especially valuable for studying AV and CDA performance in such challenging scenarios because it enables the integration of multiple simulation tools and models within a unified framework. In CDA applications, co-simulation can combine traffic simulation, vehicle dynamics simulation, vehicle control systems, and, in some cases, communication simulation to represent both subject-vehicle behavior and surrounding traffic conditions. This integrated approach allows researchers to evaluate not only whether a vehicle can successfully complete a maneuver, but also how that maneuver influences nearby traffic operations and overall system performance.

The goal of this project is to assess and demonstrate the value of co-simulation, with the potential for extension into a digital twin framework, for transportation systems management and operations (TSM&O), connected vehicle (CV), and CDA applications. The selected case study focuses on CDA operations on the approach to a freeway work zone. The specific objectives are to: (1) develop a concept and test plan for applying co-simulation and digital twins to the selected case study, and (2) demonstrate and evaluate the use of co-simulation based on the developed test plan.

The findings of this study demonstrate that co-simulation can serve as an effective tool for AV and CDA testing, particularly in complex and challenging environments such as work zones. Overall, the results indicate that co-simulation provides a practical, flexible, and scalable framework for evaluating CDA operations under realistic traffic conditions. The study further demonstrated that cooperative lane-changing behavior near work zones can be systematically assessed within a controlled simulation environment, and that the resulting performance measures can help identify system limitations and guide improvements to existing automated and cooperative driving algorithms and control logic.

The test plan and procedures were developed in accordance with the Institute of Electrical and Electronics Engineers (IEEE) standards. Although the test plan was tailored to the selected case study, it is intended to provide a generalizable framework for evaluating other automated and cooperative vehicle operations within co-simulation and digital twin environments.

The results related to the detection of work zone features, such as trucks and pedestrians, indicate reasonable agreement between the video image–based detection distances obtained from the co-simulation platform and findings reported in previous real-world studies. The study also confirmed several observations reported in the literature, including that narrower field-of-view (FOV) cameras can substantially improve object detection performance; fog conditions produce

significantly greater degradation in detection capability than rain; and larger objects, such as trucks, can generally be detected at longer distances than pedestrians.

This study evaluated the capability of co-simulation to assess the performance of CDA lane-changing strategies upstream of a work zone using the OpenCDA co-simulation platform. The evaluation considered two traffic demand levels: a low-demand condition of 1,000 vehicles/hour/lane and a high-demand condition near roadway capacity at 2,200 vehicles/hour/lane. Four merging scenarios were investigated, including a non-cooperative baseline condition and three cooperative platoon-joining strategies: cut-in joining, back joining, and front joining. The results demonstrated that both traffic demand and merging strategy significantly influenced subject-vehicle performance as well as the effects of the merging maneuvers on surrounding traffic operations.

Overall, the study showed that cooperative lane-changing strategies can substantially improve merging efficiency compared with non-cooperative automated driving behavior. However, the findings also indicated that aggressive cooperative platoon insertion using extremely short temporal gaps may introduce safety concerns and contribute to string instability, particularly under congested traffic conditions or when large speed differentials exist between the merging vehicle and platoon vehicles. Accordingly, updates to the evaluated cooperative lane-changing algorithm and its associated control parameters are recommended to reduce the acceptance of excessively short gaps that produce critically low time-to-collision (TTC) values. Cooperative merging algorithms should incorporate explicit minimum TTC and time-headway constraints relative to both lead and lag vehicles during platoon insertion maneuvers.

The analysis further identified several limitations of the evaluated cooperative control framework. The planning layer currently makes lane-changing decisions primarily based on gap availability and vehicle speed, without explicitly accounting for acceleration profiles or predicting future vehicle behavior. In addition, the tested algorithm employs a proportional–integral–derivative (PID) controller in the actuation layer, which is less advanced than control approaches such as Model Predictive Control (MPC) that are better suited for handling complex and nonlinear vehicle dynamics. Based on the test results, several additional enhancements to the lane-changing algorithm are recommended to improve both the planning and control logic of the cooperative merging process.

Infrastructure-supported merging maneuvers also have significant potential to improve operational performance and safety. For example, infrastructure-based adaptive merging strategies could be implemented according to prevailing traffic demand conditions, where the infrastructure provides guidance regarding the most appropriate merging strategy (e.g., cut-in, back joining, or front joining) together with associated operational parameters. The infrastructure could additionally provide guidance on designated lane usage for CDA platoons, recommended merge locations, dynamic updates to inter-platoon and intra-platoon gaps at specified upstream distances from the work zone, operational design domain (ODD) takeover locations for drivers, recommended CDA vehicle speeds, platoon size limitations, and other cooperative control parameters.

Future work may extend this research through the development of a digital twin framework incorporating vehicle-in-the-loop (VIL), hardware-in-the-loop (HIL), and field testing to further evaluate CDA strategies for roadway approaches to work zones with lane blockages.

Table of Contents

List of Figures

List of Tables

Abbreviations and Acronyms

AASHTO	American Association of State Highway and Transportation Officials
AV	Automated Vehicle
BSMs	Basic Safety Messages
CACC	Cooperative Adaptive Cruise Control
CARLA	CAR Learning to Act
CARMA	Cooperative Automation Research for Mobility Applications
CAVs	Connected and Autonomous Vehicles
CDA	Cooperative Driving Automation
CID	Controller Interface Device
CV	Connected Vehicle
C-V2X	Cellular Vehicle-to-Everything
DSRC	Dedicated Short-Range Communications
FDOT	Florida Department of Transportation
FHWA	Federal Highway Administration
HIL	Hardware-in-the-Loop
HMI	Human-Machine Interface
ITS	Intelligent Transportation Systems
MOSAIC	Modular Selection And Identification for Control
NS-3	Network Simulator 3
NTCIP	National Transportation Communications for ITS Protocol
OBU	Onboard Unit
ODD	Operational Design Domain
OVs	Objective Vehicles
RMSD	Root Mean Square Deviation
RSU	Roadside Unit
SAE	Society of Automotive Engineers
SIAD	Signalized Intersection Approach and Departure
SIL	Software-in-the-Loop
SNMP	Simple Network Management Protocol
SUMO	Simulation of Urban Mobility
SVs	Subject Vehicles
TraCI	Traffic Control Interface
TTC	Time To Collision
V2I	Vehicle-to-Infrastructure
V2P	Vehicle-to-Pedestrain
V2V	Vehicle-to-Vehicle
V2X	Vehicle-to-Everything
XIL	Everything-in-the-Loop
YALM	YAML Ain't Markup Language

1. Introduction

1.1 Background

Digital twin technology is an emerging area that has attracted significant interest across many disciplines, including transportation engineering. In transportation applications, a digital twin may consist of an integrated combination of enabling technologies and analytical capabilities involving cyber-physical systems, connectivity, data exchange platforms, big data analytics (including artificial intelligence (AI) and machine learning (ML)), co-simulation platforms (e.g., integrated traffic, vehicle, driving, and communication simulation), and cloud, edge, and mobile computing. Digital twins have strong potential to support intelligent transportation systems (ITS) and transportation systems management and operations (TSM&O) by enabling enhanced monitoring, testing, prediction, and operational decision making. However, additional research and demonstration efforts are needed to better establish the value of digital twins across different TSM&O and ITS applications.

The goal of this project is to demonstrate the value of a digital twin framework for a TSM&O, connected vehicle (CV), and/or cooperative driving automation (CDA) application. The primary objective is to develop, demonstrate, and evaluate a digital twin case study based on a proposed concept, as presented in Section 2.

In coordination with FDOT project management, the selected case study focuses on the use of co-simulation to evaluate CDA operations in a freeway work zone approach scenario involving a lane blockage. Although the automated vehicle (AV) within the co-simulation environment is represented digitally, the framework is intended to support future extensions to a digital twin by integrating physical transportation assets and operational data with the digital environment, as detailed in Section 2.4 of this document.

CDA enables vehicles and infrastructure to coordinate actions through machine-to-machine communication to improve transportation safety and operational efficiency (Stevens & Hopkin, 2012). With the continued advancement of connected and automated vehicle (CAV) technologies, CDA is expected to become an increasingly important component of future transportation systems. By enabling vehicles to exchange information and coordinate maneuvers, CDA has the potential to improve mobility, safety, traffic flow efficiency, and sustainability at both the individual vehicle level and the broader traffic system level.

Despite its potential benefits, widespread deployment of CDA is not expected in the near term. In addition, real-world testing, including testing at controlled facilities and test tracks, is often costly, time-consuming, and, in some cases, unsafe—particularly under complex traffic, roadway geometry, and environmental conditions such as those encountered in work zones. As a result, simulation and digital twin technologies continue to play a critical role in CDA research, development, testing, and evaluation.

Work zones present especially challenging driving environments because of lane closures, temporary traffic control changes, and the interactions among human-driven vehicles, CAV, and cooperative vehicle platoons. These conditions complicate lane-changing and merging maneuvers and may negatively affect both traffic operations and roadway safety.

For CDA-equipped vehicles to operate safely near work zones, they must first be capable of detecting relevant work zone elements, including temporary traffic control devices, workers, trucks, and other roadside or lane-blocking objects. However, AV perception performance can be significantly influenced by factors such as camera field of view (FOV), object type, and environmental conditions including rain and fog (Kim et al., 2023; Zhang et al., 2021). Evaluating detection performance under these conditions is important because perception errors or delayed detections may reduce the available response time for safe vehicle operation. Such delays can negatively affect traffic safety, roadway capacity, and traffic flow stability.

Lane-changing decision making is particularly important near work zones because lane blockages require vehicles to merge within constrained gaps, especially under higher traffic demand conditions. If the lane-changing logic does not adequately account for surrounding traffic conditions, it may result in inefficient maneuvers, increased disturbances to nearby vehicles, reduced traffic stability, and diminished safety margins. Therefore, improving lane-changing decision making and cooperative merging behavior is important for enhancing both subject-vehicle performance and overall traffic operations near work zones.

Co-simulation is particularly valuable for studying AV performance in challenging traffic environments because it integrates multiple simulation tools and models within a unified framework. In CDA applications, co-simulation can combine traffic simulation, vehicle dynamics simulation, vehicle control systems, and, in some cases, communication simulation to represent both subject-vehicle behavior and surrounding traffic conditions. This integrated capability allows researchers to evaluate not only whether a vehicle can successfully complete a maneuver, but also how that maneuver influences nearby vehicles, overall traffic operations, and traffic stability.

Among the available co-simulation platforms, the two most widely referenced open-source CDA co-simulation frameworks in the United States are CDASim and OpenCDA. These platforms provide effective environments for testing CDA applications by integrating Car Learning to Act (CARLA) and Simulation of Urban MObility (SUMO), while supporting cooperative driving functions such as platooning and cooperative merging (Dosovitskiy et al., 2017; Lopez et al., 2018; Xu et al., 2021). The platforms include core full-stack software modules representing the standard automated and cooperative driving pipeline, including perception, localization, planning, and control layers.

Despite these capabilities, limited research has examined the use of co-simulation to evaluate CDA operations under challenging conditions such as work zones while simultaneously considering perception performance, subject-vehicle behavior, and the impacts of different cooperative merging strategies on surrounding traffic.

1.2 Project Objectives

The goal of this project is to assess and demonstrate the value of a co-simulation–based digital twin framework, with the potential for extension to a fully realized digital twin, for TSM&O, CV, and/or CDA applications. The selected case study focuses on evaluating CDA operations on the approach to a freeway work zone.

The specific objectives are to:

- Develop a concept and test plan for applying co-simulation and digital twin methodologies to the selected case study.
- Demonstrate and evaluate the co-simulation framework for the case study in accordance with the developed test plan.

1.3 Report Organization

Section 2 of this document includes a discussion of the co-simulation platform used in this study and the reasons for selecting the platform. Section 3 presents the test plan developed in this study that follows the IEEE Standard for Software and System Test Documentation (IEEE Std 829-2008). Section 4 presents the results and discussion of the results. Finally, Section 5 provides conclusions and recommendations based on the study findings.

2. Co-Simulation Utilization and Test Plan

Traffic simulation tools such as PTV Vissim, Aimsun, and SUMO are widely used in both transportation research and practice for analyzing traffic operations and evaluating transportation system performance. However, traditional traffic simulation tools have limitations when evaluating emerging AV) technologies because they do not explicitly model onboard sensor behavior, perception systems, or detailed vehicle dynamics. These limitations motivate the use of co-simulation environments that integrate traffic simulation with AV simulation platforms.

The incorporation of an AV simulator within a co-simulation environment enables the evaluation of automated driving functions while accounting for the performance of onboard sensors, perception algorithms, and vehicle dynamics. When integrated with a traffic simulation model and a CDA platform, the resulting co-simulation framework allows researchers to assess not only the behavior of individual AV but also the broader impacts of AV operations on surrounding traffic flow.

Selecting an appropriate co-simulation platform is essential to achieving the objectives of this study. Initially, the research utilized the CDASim platform. However, several implementation and operational issues were identified during testing, as discussed in this section. Because resolving these issues would have required substantial modifications to the platform, the research team selected OpenCDA as the primary cooperative vehicle platform and modified the source code of OpenCDA version 0.13.0 for use in this study.

The OpenCDA co-simulation suite integrates the SUMO microscopic traffic simulator with the CARLA vehicle dynamics and sensor simulation environment while implementing CDA control algorithms. This study utilized SUMO version 1.20 and CARLA version 0.9.12 within the OpenCDA framework.

A co-simulation platform such as OpenCDA controls vehicle behavior using emulated onboard sensor data, including LiDAR, radar, and camera inputs, and allows sensor parameters to be modified to better reflect real-world sensing performance. In contrast, standalone traffic simulation tools such as SUMO do not directly model perception systems or sensor limitations. Furthermore, the co-simulation framework enables the evaluation of the impacts of environmental conditions, including rain and fog, on sensor performance and AV behavior, capabilities that are not available in conventional traffic simulation environments alone.

2.1 Co-Simulation Utilization

As stated in Section 1, The two most widely referenced open source CDA co-simulation platforms in the United States are CDASim and OpenCDA. Both are candidates for use in this project. However, there was a preference for the use of CDASim due to its additional capabilities such as the integration with communication simulation, roadside units (RSU), and signal controllers in software-in-the-loop (SIL) environments. Due to the limited experience with these platforms, the first task was to evaluate the potential of using CDASim and OpenCDA for the purpose of this project based on testing of their maturities and functionalities at the present time. This section describes the two platforms, their testing in this project, and the results of the testing used in making the decision of what platform to use.

2.1.1. CDASim System

CDASim Everything-in-the-loop (XIL) Co-simulation is an open-source, co-simulation tool developed by the Federal Highway Administration (FHWA) to advance CDA by enabling the testing of CDA platforms under different conditions.

CDASim XIL consists of the following components:

- CARMA Vehicle Control System: This is a vehicle control platform developed by FHWA, for controlling AV behaviors and incorporating CDA applications.
- Simulation Manager / Orchestrator: The co-simulation uses the multi-scale and multi-domain framework, MOSAIC, as the core runtime infrastructure and simulation manager. to synchronizes the different control systems and simulators and to manage data exchange among these systems.
- Traffic Simulator: SUMO is used as the traffic simulator to generate and assess the performance of background traffic flow and vehicle behavior.
- AV Driving Simulator: CARLA is used as the AV simulators to provide the simulation of vehicle dynamics, sensors, and 3D driving environments. CARLA simulates vehicle sensors, including cameras, LiDAR, and RADAR. It is widely used for developing and evaluating perception, planning, and control algorithms for automated vehicles.
- Communication Simulator: CDASim provides the option of integrating a communication simulator (NS-3) to simulate Vehicle-to-Everything (V2X) communications.
- CARMA Streets: This platform acts as a SIL edge-computing device (roadside equipment or RSE), allowing roadside infrastructure to communicate with vehicles and travelers.
- Virtual Traffic Signal Controller (TSC) – This a SIL signal controller application that follows the National Transportation Communications for ITS Protocol (NTCIP) interface standards.

Figure 2-1 shows the critical components of CDASim.

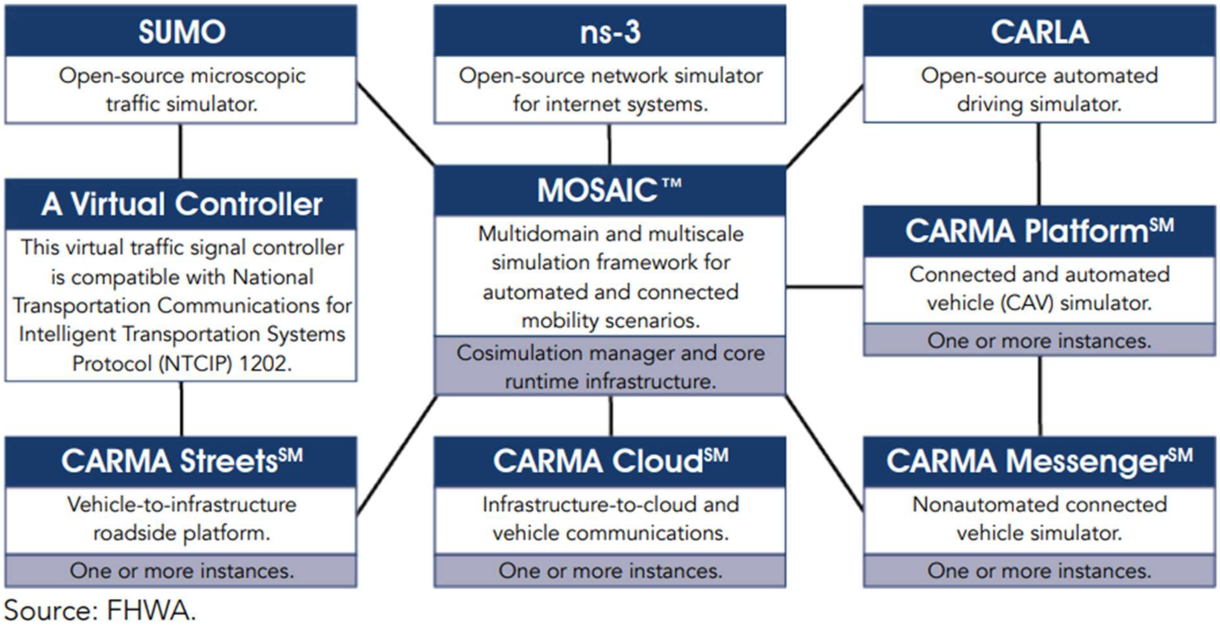

[Source: FHWA, (Federal Highway Administration, 2024)]

Figure 2-1 Components of the CDASim tool

The CARMA platform has been installed on physical real-world vehicles for research purposes. However. It can be used as a software-in-the-loop (SIL) as part of the CDASim co-simulation.

The CARMA Platform provides a flexible framework for CDA through a set of extensible application programming interfaces (APIs), including the route planning plugin API, controller plugin API, and hardware driver API. These interfaces support the integration of plugins for low-level motion planning, strategic and tactical vehicle behavior planning, and trajectory generation, enabling the testing and evaluation of automation algorithms and cooperative driving interactions. In addition, the CARMA Platform supports the composition, transmission, and reception of V2X messages in accordance with the SAE J2735 standard. By enabling cooperation among vehicles and infrastructure, the platform enhances the efficiency, safety, and overall performance of the transportation system. Figure 2-2 illustrates the key components and architecture of the CARMA Platform framework. The platform supports a range of dynamic traffic operations and cooperative driving behaviors, including yielding (slowing or stopping to avoid collisions), lane changing and merging (coordinating with surrounding vehicles to identify safe gaps), cruising (maintaining compliance with posted speed limits), platooning (supporting close-range coordinated vehicle travel), and speed harmonization (following dynamic speed guidance commands).

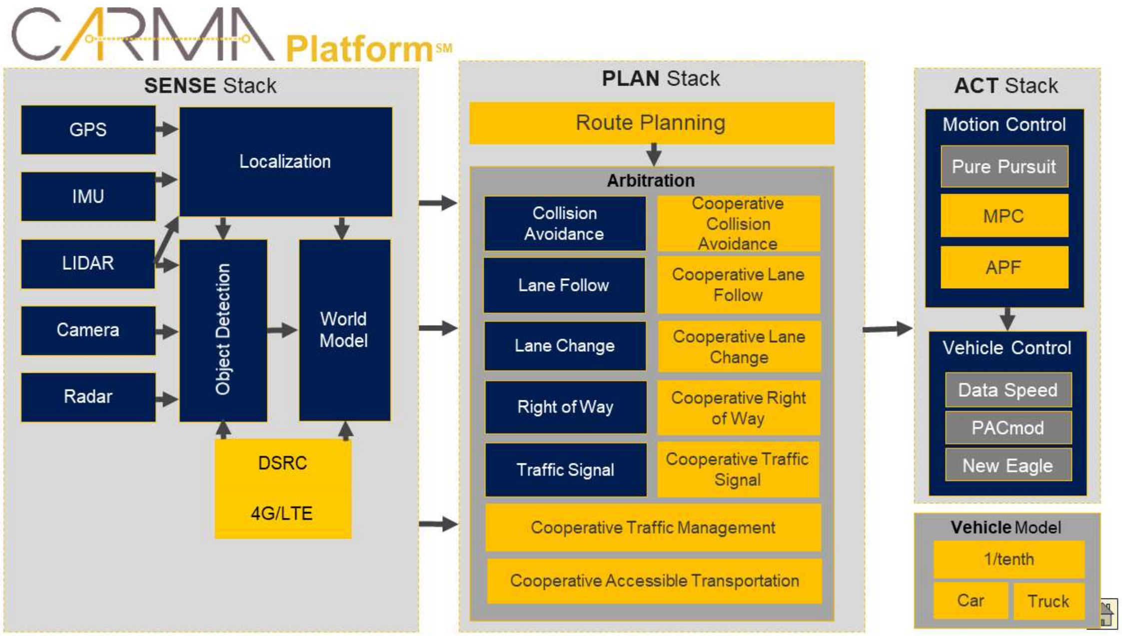

[Source: FHWA, (Federal Highway Administration)]

Figure 2-2 Key Components, Framework, and Architecture of CARMA Platform

As can be seen from Figure 2-2, CARMA consists of the following stacks:

- *The Sense Stack:* The sense stack addresses how the vehicle perceives the environment around it by using all of the sensors in the vehicle by processing and interpreting the collected data into information that can be further used to support the vehicle movement planning process.

- *The Plan Stack:* This stack is where the planning and decision-making processes take place to define the vehicle's behavior (maneuvers) and trajectory.

- *The Act Stack:* When a trajectory is generated, it is distributed to the control plugins in the Act Stack for execution. The control plugins generate the steering and speed commands needed to proceed with this trajectory and communicate these commands to the controller drivers for its execution.

- *Health Monitor:* The Health Monitor interacts with the hardware interface package and keeps track of all the device drivers and planning plugins and reports the availability of these components back to the system using an alert channel specifically designated for that purpose.

2.1.2. OpenCDA System

OpenCDA, developed by the Mobility Lab at the University of California, Los Angeles, is an open-source co-simulation platform for developing and testing CDA applications (Xu et al., 2021). It consists of three main components: traffic simulation tools, a full-stack cooperative driving system, and a scenario manager. This framework allows the testing of CDA algorithms at both the traffic level and the individual vehicle level. It supports common cooperative driving tasks such as platooning, cooperative perception, cooperative merging, and speed harmonization. The components and framework of the OpenCDA Co-simulation platform are shown in Figure 2-3.

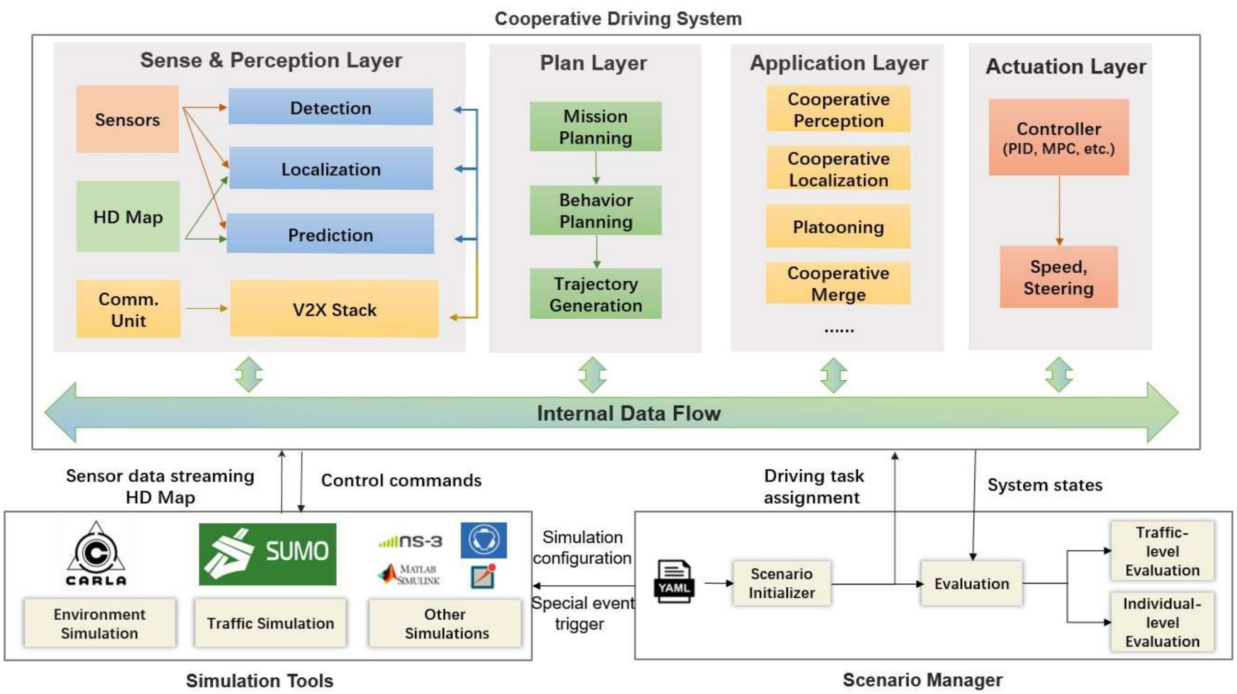

[Source: Mobility Lab, UCLA,(Xu et al., 2021)]

Figure 2-3 Components and Framework of OpenCDA Co-simulation Platform

Similar to CDASim, OpenCDA utilizes SUMO as the traffic simulation engine to provide microscopic traffic modeling for individual vehicles. SUMO enables users to create customized traffic scenarios and control vehicle behavior through the Traffic Control Interface (TraCI) API. In addition, OpenCDA integrates CARLA to provide high-quality scene rendering, realistic vehicle dynamics, and sensor simulation capabilities using the Unreal Engine framework (Epic).

When co-simulation is enabled, SUMO manages the overall traffic flow and transfers the background human-driven vehicles to the CARLA server, while CAVs controlled within CARLA interact with the surrounding traffic to perform their driving tasks. The integration of SUMO, CARLA, and OpenCDA provides a flexible and scalable environment for evaluating CDA applications under controlled traffic, roadway, and environmental conditions.

The cooperative driving system implemented in OpenCDA includes sensing, perception, planning, decision-making, and actuation functions. The platform also supports cooperative driving features defined in SAE J3216, including vehicular communication and information sharing capabilities (Cui et al., 2023). When perception is activated, simulated sensors mounted on CAVs in CARLA collect raw information from the simulated environment. Red-green-blue (RGB) cameras and LiDAR are primarily used for perception, while emulated Global Navigation Satellite System (GNSS) and inertial measurement unit (IMU) sensors are used to estimate the subject vehicle's position and motion. These sensor data are transferred to the perception layer, where surrounding vehicles, obstacles, and roadway objects are detected and localized. The perception outputs are then used by the planning and decision-making modules to determine safe vehicle behavior. In this process, the cameras provide visual information for object recognition, while LiDAR provides three-dimensional point-cloud information that supports object localization and distance estimation. If perception is not activated, OpenCDA can use ground-truth simulator information instead of sensor-based perception, which reduces perception uncertainty and simplifies the simulation. The resulting control commands are then transmitted back to CARLA, allowing CAVs to execute vehicle movements at each simulation time step.

This architecture supports both cooperative driving applications and standalone vehicle automation, making OpenCDA suitable for simulating mixed traffic environments consisting of human-driven vehicles, CVs, cooperative automated vehicles, and fully AVs. In OpenCDA, cooperation among AVs is implemented at the application layer, where CDA-enabled vehicles exchange status and intent information through the V2X communication stack. This shared information enables vehicles to coordinate and agree on cooperative maneuvers such as platoon formation, cooperative lane changing, and merging operations.

The Scenario Manager module in OpenCDA is responsible for scenario configuration, initialization, event management, and performance evaluation. Users configure simulation scenarios using a YAML Ain't Markup Language (YAML) file based on the OpenCDA configuration template. YAML is a human-readable data serialization format commonly used for configuration management (Yaml, 2023). The configuration file defines CARLA server settings, traffic flow characteristics, roadway configurations, and CAV parameters. The Scenario Manager loads the configuration file, retrieves the required parameters, and communicates them to the CARLA server to generate traffic flow and create a Vehicle Manager instance for each CAV in the simulation.

An example of a platooning scenario operating under the OpenCDA co-simulation framework is illustrated in Figure 2-4 (Xu et al., 2021). The Figure 2-4 (a) shows the traffic simulation environment in SUMO, while the Figure 2-4 (b) presents the corresponding view in CARLA, including the planned vehicle trajectory represented by green lines and trajectory points represented by red markers. The Figure 2-4 (c) displays the RGB camera image and three-dimensional (3D) LiDAR point cloud collected by the onboard sensors installed on the CAV. The illustrated example uses a customized benchmark roadway network representing a basic freeway merge segment consisting of a two-lane freeway and a single-lane entrance ramp.

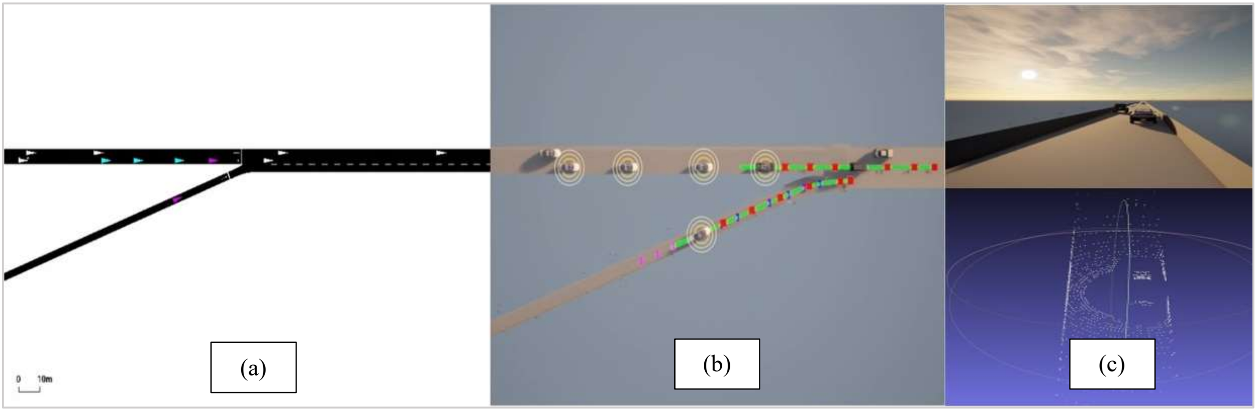

[Source: Mobility Lab, UCLA,(Xu et al., 2021)]
Figure 2-4 Screenshots of Running Platooning Scenario in OpenCDA (Xu et al., 2021)

2.1.3. Assesment of CDA Platforms

As described in the above subsections, CDASim and OpenCDA are both open-source platforms designed for supporting CDA research, development, and testing. However, they differ in that CDASim has more focused on simulating high-fidelity integration with infrastructure components such as V2X communications, roadside equipment, and signal controllers. Table 2-1 provides a comparison between the usability and functionality of the two platforms. Based on Table 2-1, it can be seen that the FHWA CDASim allows more detailed testing of the integration with infrastructure components, while OpenCDA emphasizes faster prototyping and experimentation.

Table 2-1 Comparison of CDASim and OpenCDA Features

Feature	CDASim	OpenCDA
Core Components	CARLA, SUMO, NS-3, MOSAIC, CARMA, CARMA Street, Virtual Controller	CARLA and SUMO
Communication Modeling	V2X simulation using NS-3	Software-level message exchange framework through Python-based communication modules using middleware abstractions
Infrastructure Integration	Roadside connected vehicle equipment and controllers	Emulated equipment and controllers
CDA Vehicle Software Stack	CARMA	Python-based prototype stack
Ease of Setup	More complex. Documentation and tutorials are not sufficient at the present time.	Easier
Learning Curve	Steep.	Moderate
Computational Demand	Higher	Lower

Given CDASim's strengths in providing realistic infrastructure-integrated testing and its clear pathway toward future integration with physical vehicles, the platform was selected as the preferred solution for this project. However, the research team encountered challenges in two primary areas while attempting to deploy and use the system.

First, significant difficulties were encountered during the installation and configuration process. Establishing a fully operational version of CDASim was challenging due to the complexity of the platform and its numerous dependencies. After multiple installation attempts and extensive coordination with the platform support team, the research team was ultimately able to achieve a functional deployment.

Second, issues were faced when running CDASim such as having CARMA vehicles not spawning, spawn vehicles not moving, and spawn vehicles not following the desired route. Although some of the technical issues were resolved, challenges remained in producing realistic lane-changing behavior for CDA vehicles approaching work zones.

2.2 Concept of Operations

This section presents a concept of operations (ConOps) of the co-simulation/digital twin capability for CDA driving and its use in the case study of this report.

2.2.1. Purpose

The purpose of this ConOps is to define the use of a co-simulation environment that can be progressively extended into a digital twin framework for the testing, evaluation, and validation of CDA applications. The initial application presented in this study focuses on CDA operations approaching freeway work zones with lane closures, where complex interactions among human-driven, connected, automated, and cooperative vehicles create challenging operating conditions. The concept is generalizable and can be applied to CDA applications in a broad range of transportation environments.

The proposed concept integrates multiple simulation platforms into a unified, synchronized environment capable of representing vehicle behavior, traffic operations, and system-level interactions under realistic operating conditions. This integrated co-simulation framework enables the evaluation of individual vehicle performance as well as the operational impacts of cooperative driving strategies on the surrounding transportation system. While the initial implementation is conducted entirely within a virtual environment, the architecture can support a phased transition to a fully operational digital twin. Future implementations can incorporate physical roadside infrastructure, onboard vehicle systems, connected and automated vehicles, communication networks, and other field assets through continuous data exchange and synchronization between the physical transportation system and its digital representation.

2.2.2. **Vision**

The capability envisioned by this concept is to provide a comprehensive testing and evaluation environment that complements controlled test-track facilities, such as SunTrax, and real-world field testing for the development, testing, evaluation, and validation of automated and cooperative driving systems. By using a co-simulation environment, challenges associated with physical testing can be addressed while enabling assessment of system performance under a wide range of operating conditions. The proposed environment can capture the complex interactions among human-driven vehicles, CVs, AVs, CDA vehicles, roadway infrastructure, communication systems, and other road users, including pedestrians and cyclists. This enables researchers to evaluate the performance of automated and cooperative driving functions but how these functions influence and are influenced by surrounding traffic conditions, infrastructure operations, and TSM&O strategies. Although the initial implementation is intended as a virtual co-simulation environment, the architecture can support a phased evolution toward a transportation digital twin.

2.2.3. **Operational Objectives**

The objectives of the utilization of the simulation-based environment explored in this study are to:

- Evaluate CDA performance under complex traffic conditions.
- Evaluate the ability of simulation to assess the detection of surrounding features under different weather and lighting conditions
- Evaluate the ability of the developed environment to simulate cooperative lane-changing and merging in the approach to freeway work zones.
- Demonstrate the utilization of the results to quantify operational impacts on the subject CAV and surrounding traffic.
- Establish the technical foundation for digital twin implementation.

2.2.4. **Operational Scenarios**

The case study consists of a freeway work zone where one or more lanes are closed. As traffic approaches the work zone, the utilized environment simulates traffic conditions upstream of the infrastructure. Information is available to the vehicle through their on-board sensors, vehicle-to-infrastructure (V2I) communication, and vehicle-to-vehicle (V2V) communication. Utilizing this information, the vehicle controllers execute lane-change decisions. The traffic simulation updates the impacts on surrounding vehicle behaviors and provide the opportunity to evaluate maneuver feasibility. Finally, the individual vehicle performance and system performance are recorded and analyzed. The details of the specific scenarios utilized in this study are presented as part of the Test Plan in Section 3 of this document.

2.2.5. **Stakeholders**

The primary stakeholders of the environment explored in this study include the FDOT and other state DOTs, local agencies counties, TSM&O practitioners, researchers and developers, and test track facilities managers and staff.

2.3 Co-Simulation and Digital Twin Framework

The Co-Simulation and Digital Twin framework consists of six components that collectively support testing, evaluation, and future digital twin deployment.

- Scenario Definition: This layer defines the evaluated scenario including roadway geometry, work zone configuration, traffic demand, vehicle composition, environmental conditions, and performance measures
- Co-Simulation Environment: This environment includes two or more simulation engines executed simultaneously through a synchronization manager. At a minimum, this environment includes a traffic simulation tool, a vehicle dynamics simulation and automatic vehicle simulation tool, and a synchronization manager and data exchange middleware.
- Cooperative Driving Functions: These functions built in the environment provide the automated and cooperative driving tasks including detection, perception, prediction, motion and trajectory planning, and vehicle control. These functions allow gap assessment, car-following lane-change planning, platoon coordination and joining maneuvers, and infrastructure interaction
- Performance Assessment: The environment utilizes simulation outputs to estimate the values of traffic and individual vehicle performance measures, as identified in the Test Plan.
- Decision Support: This component utilizes the performance measures based on simulation outputs to provide actionable information regarding the ability of the tested automated control to execute the dynamic driving task under different operations design domain (ODD) with and without cooperation, the benefit of infrastructure-vehicle and vehicle-everything cooperation, and the impact of TSM&O strategy interaction with the automated driving systems and CDA.
- Digital Twin Extension: The sixth component not tested in this study enables migration toward a full digital twin environment as described in the next section.

2.4 Digital Twin Extension

A future effort could extend the co-simulation environment developed in this study into a fully functional transportation digital twin by integrating physical transportation assets and operational data with the digital environment. A digital twin maintains a continuously synchronized representation of the physical transportation system through the exchange of real-world data. For CDA applications, the digital twin represents not only individual vehicles but, more importantly, the interactions among vehicles, roadway infrastructure, communication networks, traffic operations, and work zone conditions. Depending on the intended application, the digital twin may include physical CAVs, roadside units (RSUs), onboard units (OBUs), traffic sensors, traffic signal controllers, work zone devices, traffic management systems, and other connected infrastructure.

Each physical asset incorporated into the digital twin is associated with a corresponding digital representation capable of reproducing its operational state and behavior. Physical assets continuously provide observations that update their digital counterparts, while the digital environment performs simulation, analytics, and predictive assessments using the synchronized system state. Depending on the application, the digital twin may also provide recommendations or control actions to physical systems, establishing a bidirectional information exchange between the physical and digital environments.

The digital twin may ingest information from multiple data sources. For CV applications, these data may include Basic Safety Messages (BSMs), Signal Phase and Timing (SPaT) messages, MAP messages, Traveler Information Messages (TIMs), and other CV communications. Vehicle state information may be obtained from onboard systems, including Global Navigation Satellite System (GNSS) receivers, Inertial Measurement Units (IMUs), Controller Area Network (CAN) data, wheel-speed sensors, steering angle sensors, and other vehicle telemetry. Infrastructure data may include traffic detector measurements, signal controller status, roadside sensor observations, work zone device status, weather information, and traffic management center data. In addition to receiving operational data from the field, the digital twin may transmit recommended signal timing plans, active traffic management parameters, cooperative driving advisories, or other operational guidance back to the physical transportation system.

Establishing a robust and secure data integration pipeline is fundamental to maintaining an operational digital twin. The communications architecture should support reliable data acquisition, validation, time synchronization, storage, and distribution using proven middleware and communication technologies appropriate for connected transportation systems. Each observation should be assigned an accurate timestamp to ensure consistent temporal alignment across all participating subsystems and to support the synchronization of distributed data sources.

Continuous synchronization between the physical transportation system and its digital representation is a basic characteristic of a digital twin. This synchronization includes spatial synchronization, which maintains the correspondence between the physical and digital locations of vehicles and infrastructure assets; temporal synchronization, which ensures that all system components operate using a common time reference; and state synchronization, which continuously updates the operational state of digital models using observed field data. The required synchronization frequency depends on the intended application. For example, vehicle control and cooperative driving functions may require synchronization intervals on the order of tens of milliseconds, whereas TSM&O applications, may operate effectively with updates every few seconds.

3. Test Plan

This section presents the test plan developed in this study to assess and demonstrate the use of co-simulation for evaluating the operation of CDA vehicles approaching a work zone with a lane blockage. The test plan includes a description of the selected use case, the systems and components under test, the operational design domain (ODD), test objectives and performance metrics, test scenarios, and testing procedures. The test plan was developed in accordance with the IEEE *Standard for Software and System Test Documentation*, specifically the 2008 revision of IEEE Std 829-1998 (Ieee, 2008).

Although the test plan was developed specifically for the selected case study, it is intended to serve as a model framework for evaluating other automated and cooperative vehicle operations within co-simulation and digital twin environments.

3.1.1. Use Case Description

The use case examined in this study involves the merging maneuvers of a single AV into either a CDA platoon or a traffic stream of human-driven vehicles while approaching a work zone with a one-lane blockage. In these scenarios, the AV performs lane changes from the blocked lane to an adjacent open lane in response to the work zone configuration. The test evaluates the effects of this lane-change maneuver on both the subject AV and the surrounding traffic, including impacts on vehicle interactions, traffic operations, and merging behavior.

The testing and evaluation framework compares two types of vehicle automation systems. The first is an automated driving system (ADS)-equipped vehicle that relies solely on onboard sensors—such as cameras, LiDAR, and radar—to collect and process information through its perception system in order to perform driving tasks and execute lane changes independently, without cooperation from other vehicles or infrastructure. The second is a CDA-equipped vehicle, which utilizes connectivity and coordination with other vehicles in addition to data obtained from onboard sensors. This cooperative approach enables vehicles to exchange information and coordinate maneuvers more effectively in complex driving environments.

3.1.2. Tested Units

The units under test include a single AV traveling in the blocked lane and attempting to perform a lane-change maneuver, as well as either human-driven vehicles or CDA vehicle platoons operating in the adjacent open lane, depending on the scenario. In addition, infrastructure support components capable of providing infrastructure-to-vehicle (I2V) information, guidance, or control may be incorporated based on the specific test scenario.

All vehicles used in the current study are virtual vehicles generated within the co-simulation environment. However, in a digital twin implementation, these virtual vehicles could be replaced or supplemented by physical vehicles operating within a VIL framework. The following sections provide a description of the tested units.

- Subject Vehicle (SV): The subject vehicle is an AV, with or without cooperative driving capabilities, traveling in the right lane of a three-lane freeway segment where the right lane is blocked downstream due to a work zone. The vehicle attempts to merge into the adjacent open lane upstream of the lane blockage, when feasible, by joining a platoon or traffic stream approaching the work zone in the adjacent lane. Within the co-simulation environment, the SV is generated and controlled by CARLA and synchronized with traffic operations modeled in SUMO. It is assumed that the AV operates at SAE automation Level 3 or higher, in accordance with SAE J3016 standards, and, when cooperative capabilities are enabled, CDA Class C or higher according to SAE J3216 standards.

- Object CDA Vehicles (CDA-OVs): These are CDA vehicles operating as part of a platoon in selected test scenarios on the adjacent open lane (i.e., the middle lane of the three-lane freeway segment approaching the work zone). In these scenarios, the SV traveling in the blocked lane attempts to perform a lane-change maneuver and merge into the platoon upstream of the lane blockage. Vehicles within the platoon follow one another based on the cooperative driving algorithms implemented within the co-simulation platform (OpenCDA). The CDA-OVs are generated and controlled by CARLA and synchronized with traffic operations modeled in SUMO. It is assumed that the CDA-OVs operate at SAE automation Level 3 or higher, in accordance with SAE J3016 standards, and meet CDA Class C or higher requirements according to SAE J3216 standards.

- Human-Driven Object Vehicles (HV-OVs): These are human-driven vehicles (HVs) traveling in the same lane and adjacent lanes as the subject vehicle (SV) while approaching the work zone. The HV-OVs are generated and managed by the traffic simulator within the co-simulation platform (SUMO in this study) and synchronized with the AV simulator (CARLA). The HV-OVs operate according to the built-in car-following and lane-changing behavior models implemented in SUMO, representing conventional human driving behavior within the simulated traffic environment.

- Infrastructure Support Component: This component can be introduced in some scenarios. Infrastructure support is the management component of the co-simulation environment, responsible for the provision of information. guidance, or control to the SV and CDA-OVs during the merging of the SV lane. This component was not tested in this study. However, recommendations for its introduction are provided in the recommendation section.

3.1.3. Operational Design Domain (ODD)

The ODD defines the operating environment assumed for the test scenarios, including roadway characteristics, traffic conditions, lane and shoulder closures, pavement conditions, and environmental factors such as lighting, sun position, and weather conditions.

The simulations were conducted on a straight and level four-lane arterial roadway segment with clearly visible lane markings. Traffic conditions included multiple demand levels representing different congestion states. The baseline scenario assumed daytime operation under clear-sky and dry pavement conditions with no adverse effects from sun glare or shadowing. Additional scenarios were evaluated under adverse weather conditions, including heavy rain and fog, to assess system performance under reduced visibility and degraded environmental conditions.

3.1.4. Test Objectives and Performance Metrics

The test objectives and associated evaluation metrics are provided below. These objectives focus on assessing the use of co-simulation to evaluate CDA performance in a work zone approach scenario involving lane blockage. Although the AV in the co-simulation is represented digitally, the framework is intended to support future extensions that incorporate a physical vehicle in the loop and testing on test track.

Objective 1: Evaluate the capability of the co-simulation platform to assess the performance of the onboard sensing systems of AVs to detect work zone features under different operating conditions, including changes in camera FOV and adverse weather conditions.

- **Detection Distance:** This is the distance at which the probability score assigned by the object detection model to the presence of an object exceeds a certain threshold (60% was used in this study). Higher distances indicate earlier detection and thus response to features such as those of work zones. In this study, confidence values were used to evaluate how object detection reliability varies.

- **Precision** measures the proportion of correct detections among all reported detections and reflects the accuracy of the model's predictions. A high precision value indicates that the model generates fewer false positives and is therefore less likely to incorrectly classify non-work zone objects as relevant hazards. Precision is calculated as shown in Equation 1.

$$\text{Precision} = \frac{\textit{True Positives}}{\text{True Positives} + \text{False Positives}} \tag{1}$$

- **Inference time (ms)** represents the computational time required by the detection model to process one frame and produce an output. This is one of the most important performance measures for onboard video-based object detection systems in AVs because it directly affects the ability of the vehicle to perceive, react to, and safely respond to its environment in real time. In automated driving applications, perception algorithms must operate continuously on streaming sensor data while maintaining sufficiently low latency to support safe vehicle control decisions.

Objective 2: Evaluate the ability of the platform to assess safe and efficient lane-change maneuvers by CDA-equipped vehicles in the approach to a work zone lane blockage.

- The **Lane-change completion time (s):** This variable measures the time required for the subject vehicle to complete a lane-change maneuver. It is defined as the time from the start of the lateral movement until the vehicle finishes the maneuver.

- The **Gap acceptance distance (ft):** This variable describes the observed spacing (distance gap) between the subject vehicle and the lead and lag vehicles in the target lane at the start of the lane-change maneuver.
- **Time-to-collision (TTC) (sec):** This is a surrogate safety measure that quantifies the time remaining before two vehicles would collide if they continued traveling at their current speeds. In this study, TTC was calculated with respect to both the lead and lag vehicles in the target lane using Equation 2.

$$\mathrm{TTC_{Break}(t)} = \frac{x_{i-1}(t) - x_i(t) - \bar{L}}{v_i(t)} \tag{2}$$

where $\mathrm{TTC_{Break}}(t)$ is the time to collision value of vehicle i at time t, x_i (t) is the position of vehicle i at time t, x_{i-1} (t) is the position of vehicle i-1 at time t, v_i (t) is the speed of vehicle i at time t, and L is the average length of vehicles.

- **Vehicle acceleration (ft/s^2) and Jerk (ft/s^3):** These are variables used to evaluate the dynamic response of the subject vehicle during the lane-change maneuver. Higher values indicate unsafe and potentially instable conditions.
- **Speed differential at merge point (ft/sec)**: This variable involves a comparison between the speed of the SV (the merging vehicle) and the speeds of the lead and lag vehicles at the location and time of completing the merging.

Objective 3: Assess the impact of merging with and without cooperation on the performance of surrounding vehicles.

- The **standard deviation of speeds across vehicles (SDt):** This variable measures the variation in speed among vehicles of a traffic stream for the time from the start of the lane change maneuver until 10 seconds after the lane change is complete. This metric reflects the degree of speed inconsistency across the traffic stream and is calculated as shown in Equation 3.

$$\mathrm{SDt} = \sqrt{\frac{1}{n-1}\sum_{i=1}^{n}(V_i - \bar{V})^2} \tag{3}$$

where n is the number of vehicles, V_i is the speed of vehicle i, and $\bar{V}$ is the mean speed of all vehicles.

- The **standard deviation of speed over time for individual vehicles (SDv):** This variable measures the temporal fluctuation in the speed of each vehicle as it travels through the analysis region and is calculated as shown in Equation 4.

$$\mathrm{SDv} = \sqrt{\frac{1}{n_1-1}\sum_{j=1}^{n_1}\left(S_j - \bar{S}\right)^2} \tag{4}$$

where n_1 is the number of speed observations collected for a specific vehicle, S_j is the speed of the vehicle at interval j, and $\bar{S}$ is the mean speed of that vehicle over the analysis period.

- The **percentage of oscillating vehicles (%):** This variable is the proportion of vehicles that experienced at least one oscillation within the analysis region. An oscillation was identified when a deceleration phase is followed by an acceleration phase based on the smoothed acceleration profile.

- The **Lag vehicle maximum deceleration (ft/s²):** This variable is defined as the highest deceleration experienced by the lag vehicle during the analysis period. This metric was used to measure the direct effect of the merging maneuver on the following vehicle in the target lane. Larger negative values indicate that the lag vehicle had to slow down more sharply.

3.2 Test Scenarios

Different test scenarios are identified for the testing of the objective as described below.

Objective 1 – Work Zone Feature's Detection Performance

Among different object detection algorithms, the You Only Look Once (YOLO) image processing models have been widely used in AV applications for object detection based on onboard camera images. These algorithms utilize convolutional neural networks and have to be trained before using them in real-time detection of objects such as vehicles, pedestrians, and roadway features or obstacles (Benjumea et al., 2021; Dazlee et al., 2022; Hsu & Lin, 2021; Lan et al., 2018; Li et al., 2021; Liang et al., 2022; Terven & Cordova-Esparza, 2023). In this study, the YOLOv5s and YOLOv8s generations of YOLO were used in the detection. Both models were pretrained on the COCO dataset, which is a large-scale annotated dataset commonly used for object detection tasks (Lin et al., 2015). YOLOv5 (Jocher, 2020) is an open-source object detection framework developed and maintained by Ultralytics, and it has been widely used due to its balance between detection accuracy and inference speed. YOLOv8 (Jocher et al., 2023) introduced newer architecture and supports multiple computer vision tasks, including object detection, segmentation, pose estimation, tracking, and classification.

The small versions of both models were used because they require lower computational resources and are more suitable for real-time vehicle-based detection applications. Comparing YOLOv5s and YOLOv8s allows this study to evaluate whether the newer YOLOv8s model improves detection performance under different camera FOV and weather conditions compared with YOLOv5s. **Error! Not a valid bookmark self-reference.** summarizes the test scenarios used for objective 1. These scenarios involve different YOLO models, FOV, and weather conditions, including sunny, rainy, and foggy environments. Details of the weather variation are described in Section 3.7.4 Co-simulation Modeling.

Table 3-1 Test Scenarios for Objective 1

Scenario	YOLO Model	FOV	Weather Condition
1-1	YOLOv5s	90°	Sunny
1-2	YOLOv5s	45°	Sunny
1-3	YOLOv5s	45°	Rain
1-4	YOLOv5s	45°	Fog
1-5	YOLOv8s	90°	Sunny
1-6	YOLOv8s	45°	Sunny

Scenario	YOLO Model	FOV	Weather Condition
1-7	YOLOv8s	45°	Rain
1-8	YOLOv8s	45°	Fog

Objectives 2 and 3 - Impacts on Subject Vehicles and Object Vehicles (Surrounding Vehicles)

Table 3-2 summarizes the scenarios used for the tests associated with objectives 2 and 3. The scenarios are defined based on traffic demand level and merging strategy. These scenarios were designed to evaluate merging performance under different demand conditions and cooperation strategies.

Table 3-2 Test Scenarios for Objectives 2 and 3

Scenario	Demand (vehicles/hour/lane)	Merging Strategy
2-1	1,000	No cooperation
2-2	1,000	Cut-in joining
2-3	1,000	Back joining
2-4	1,000	Front joining
2-5	2,200	No cooperation
2-6	2,200	Cut-in joining
2-7	2,200	Back joining
2-8	2,200	Front joining

3.3 Test Procedures

This section describes the test procedures used to apply a co-simulation framework to evaluate CDA operations in the approach to a work zone with lane blockage. The analysis focuses on the three main objectives related to work zone object detection, lane-change and merging performance of the subject vehicle, and the impacts of the merging maneuver on the surrounding traffic.

3.3.1. Study Area

The roadway network used in this project was consistent across all study objectives. The study area consists of a four-lane arterial roadway segment with a right-lane closure upstream of a stationary work zone. The roadway segment is approximately 2,500 ft long, and the work zone is located in the rightmost lane approximately 2,100 ft downstream from the segment starting point, as illustrated in Figure 3-1. The work zone configuration was designed to represent a typical lane blockage condition requiring vehicles in the closed lane to merge into the adjacent lane upstream of the work zone.

For objective 1 testing, the SV was initially positioned in the second lane approximately 590 ft upstream of the work zone elements. This configuration was used to evaluate AV detection and perception performance in the vicinity of the work zone.

For objectives 2 and 3, the SV was positioned farther upstream in the rightmost lane at the beginning of the roadway segment. This configuration allowed the SV to approach the work zone, execute the required lane-change maneuver, and interact with surrounding traffic under different cooperative and non-cooperative merging strategies.

Figure 3-1 Study area

3.3.2. Platoon Formation, Lane Changing and Merging Mechanisms

OpenCDA contains built-in applications for platooning, lane changing, and cooperative merging (Lab, 2024). These built-in applications were used and modified in this study. In the merging process, the single CDA vehicle continuously searches for an opportunity to join a platoon. Once the single CDA vehicle comes within a specified V2V communication range of a platoon, it sends a merging request. The platoon then accepts or rejects the request based on factors such as the maximum allowed number of platoon members, inter-vehicle gap, and speed difference. The destination of the single CDA vehicle and the available gap in the adjacent lane govern most of the lane-changing behavior. The single CDA vehicle can join a platoon in three ways: front joining, back joining, and cut-in joining. In front joining, the single CDA vehicle changes speed to merge in front of the platoon to become the new leader. In back joining, the single CDA vehicle merges behind the vehicles in the platoon to become the last follower. In the cut-in joining, the existing platoon members adjust their speeds to create a gap so that the single CDA vehicle can merge into the middle of the platoon.

To support these maneuvers, the system allows adjusting parameters such as platoon speed, inter-vehicle gap, maximum platoon size, and the maximum speed of the single merging CDA vehicle during the merge. In this study, the platoons were spawned in the middle lane and were restricted from changing lanes, while the merging CDA vehicle operated in the rightmost lane and allowed them to travel freely before merging into the platoon. Restricting the platoon on operating on the open lanes ahead of the work zone could be used as an infrastructure-based strategy to reduce the impact of lane changing behaviors ahead of the work zone.

3.3.3. Co-simulation Modeling

This section describes how the co-simulation platform was used in this study to conduct testing in accordance with the test plan objectives.

Objective 1 – Work Zone Feature's Detection Performance

The first objective was to evaluate the ability of the co-simulation platform to assess the detection of work zone features. The two object detection models utilized in this study (YOLOv5s and YOLOv8s) were tested under different environmental and camera settings. The analysis focused on detecting two object classes from the COCO dataset, pedestrian and truck, which represent critical work zone features, as shown in **Error! Reference source not found.**-2.

Figure 3-2 Pedestrian and Truck Objects used for Object Detection esting

An RGB camera sensor was attached to the ego vehicle to capture images for object detection. The camera was positioned in front of the subject vehicle. The camera resolution was set to 640 × 640 pixels, and two FOV settings, 45° and 90°, were tested to evaluate the effect of viewing angle on detection performance. The camera operated using the default simulation time step.

CARLA allows the simulation of different weather conditions, including rain and fog. This feature makes it possible to evaluate the effect of adverse weather on perception performance in a controlled environment. Although CARLA does not allow direct input of exact real-world weather parameters such as rainfall intensity in mm/hr, it allows users to modify weather intensity values using percentage-based parameters. In this study, weather settings were selected to represent clear, rainy, and foggy conditions.

Based on the findings of Bi et al. (Bi et al., 2022), 100% precipitation intensity in CARLA approximately corresponds to 50 mm/hr of rainfall, while 100% fog intensity is comparable to about 1 g/m^3 of fog water content. Therefore, these settings were used to represent heavy rain and dense fog conditions in the sensor impact study.

Error! Reference source not found.-3 summarizes the weather parameters used for the sensor impact testing. Figure 3-3 shows visualizations of the tested conditions. The weather scenarios used in this study are defined as follows:

- Sunny: clear weather conditions
- Rainy: heavy rain conditions corresponding to approximately 50 mm/hr
- Foggy: dense fog conditions corresponding to approximately 1 g/m^3

Table 3-3 Utilized Weather Parameters for Sensor Performance Testing

Parameters	Sunny	Rainy	Foggy
Cloudiness, %	0	50	0
Precipitation, %	0	100	0
precipitation deposits, %	0	100	0
Wetness, %	0	100	0
Fog, %	0	0	100

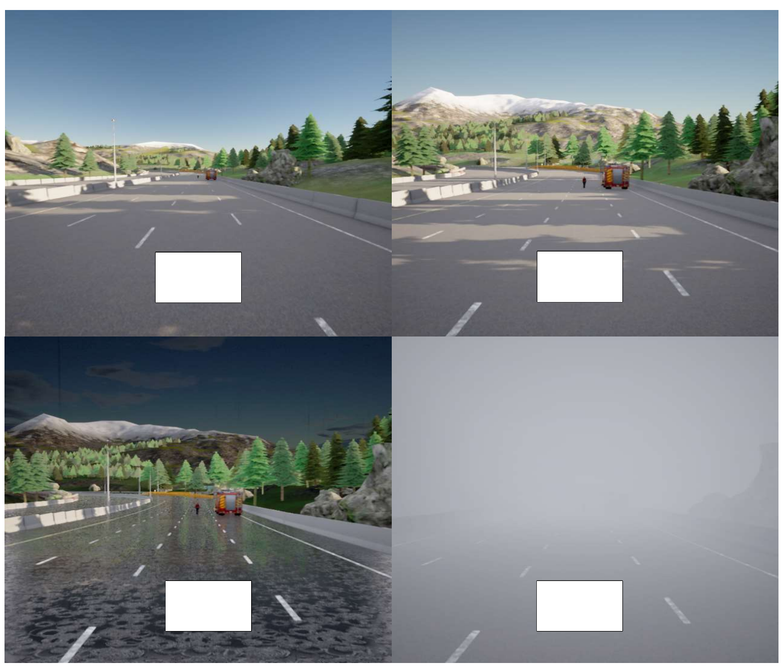

Figure 3-3 Sensor Testing Under Different Weather Conditions: (a) FOV90 Sunny, (b) FOV45 Sunny, (c) FOV45 Rain and (d) FOV45 Fog.

After the simulation was completed, sensor data were collected from CARLA using Python scripts. These data included the camera images, detection outputs, confidence values, and inference times.

Objectives 2 and 3 - Impacts on Subject Vehicles and Object Vehicles (Surrounding Vehicles)

For objectives 2 and 3, the same co-simulation environment was used to evaluate lane-changing performance and the effects of merging maneuvers on surrounding traffic under varying traffic demand levels and merging strategies. The roadway geometry and work zone configuration were identical to those described in the study area section.

The test scenarios differed according to traffic demand level and merging strategy. Two traffic demand levels were considered: 1,000 vehicles/hour/lane and 2,200 vehicles/hour/lane. The merging strategies evaluated included no cooperation, cut-in platoon joining, back platoon joining, and front platoon joining. These conditions were specified through the configuration files of the co-simulation platform. Weather conditions were maintained as clear for all scenarios, while all other simulation parameters remained at their default settings.

Human-driven vehicles (HVs) were generated within the simulation model based on the selected traffic demand and were randomly distributed across all lanes. The movements of CAV were controlled through CARLA, whereas the movements of HVs were controlled through SUMO. This configuration enabled realistic interactions between automated and human-driven vehicles within the work zone environment.

Upon completion of the simulation experiments, the resulting data were collected and processed to evaluate both SV performance and surrounding traffic performance under the different test scenarios. Vehicle trajectory outputs from SUMO were exported in XML format and converted to CSV files using a Python-based post-processing script. The script extracted time-dependent vehicle attributes, including position, speed, acceleration, lane assignment, and leader-related information. The processed CSV files were subsequently used to compute the performance measures described in the following section.

4. Results and Discussion

This chapter reports and discusses the results of the analysis performed in this study to demonstrate the use of co-simulation analysis according to the test plan presented in the previous chapter.

4.1 Evaluation of the Co-simulation Platform for Work Zone Presence Detection

This section presents the results of the investigation into the ability of the co-simulation environment to simulate work zone presence detection. As discussed in Chapter 2, work zone detection was performed within CARLA using trained machine vision algorithms (YOLOv5s and YOLOv8s) under varying FOV configurations and weather conditions. The evaluation was conducted using three primary performance metrics: detection confidence, precision, and inference time.

4.1.1. Detection Distance Analysis

Table 4-1 summarizes the distance from the work zone, in feet, at which the detection confidence first reached a specific threshold (60% confidence was used in this study) under different environmental and camera configurations. The baseline condition consisted of the YOLOv5s algorithm operating with a 90° FOV under sunny weather conditions.

Table 4-1 Distance from Work Zone in feet at which the Detection Confidence Reached 60%

Object	**YOLO Model**	**FOV 90 Sunny**	**FOV 45 Sunny**	**FOV 45 Rain**	**FOV 45 Fog**
Pedestrian	YOLOv5s	115.32 ft	225.33 ft	171.52 ft	83.43 ft
	YOLOv8s	74.38 ft	203.90 ft	183.14 ft	83.96 ft
Truck	YOLOv5s	144.32 ft	290.19 ft	146.46 ft	36.45 ft
	YOLOv8s	135.17 ft	307.74 ft	237.83 ft	N/A

For pedestrian detection, the baseline configuration achieved 60% confidence at a distance of 115.32 ft from the work zone. When the FOV was narrowed from 90° to 45° using YOLOv5s under sunny conditions, the detection distance increased to 225.33 ft, indicating improved detection performance associated with the increased camera coverage and enhanced visual focus. Under the 45° FOV configuration, adverse weather conditions reduced the detection distance relative to the sunny condition. Specifically, the confidence threshold was reached at 171.52 ft during rain conditions and at 83.43 ft during fog conditions. These results indicate that rain, and especially fog, negatively affected detection performance. Compared with the baseline condition, the YOLOv8s algorithm operating under sunny conditions with a 90° FOV reached the confidence threshold at a shorter distance of 74.38 ft. This result suggests lower pedestrian detection confidence for YOLOv8s relative to YOLOv5s under the same FOV and weather conditions.

For truck detection, the baseline condition (YOLOv5s with a 90° FOV under sunny conditions) achieved the confidence threshold at a distance of 144.32 ft from the work zone. Narrowing the FOV to 45° while using YOLOv5s under sunny conditions increased the detection distance to 290.19 ft, demonstrating that the narrower FOV substantially improved truck detection performance. Among all tested scenarios, YOLOv8s operating under sunny conditions with a 45° FOV achieved the best performance, reaching the confidence threshold at the longest distance of 307.74 ft. Under rainy conditions, YOLOv8s reached the threshold at 237.83 ft, compared with 146.46 ft for YOLOv5s, indicating that YOLOv8s provided greater robustness for truck detection in rain. Although trucks are expected to be detected at longer distances than pedestrians, YOLOv5s detected the truck at a shorter distance than the pedestrian under rainy conditions, as seen in Table 4-1. Examination of the animation showed that the truck appeared darker under rain and wet-road conditions. Reflections from the wet pavement and rain effects may have made the truck less distinguishable from the background, which may have lowered YOLOv5s detection confidence. This indicates the potential need to train the detection algorithm under different weather conditions to account for the rain and wet pavement effects. Under foggy conditions, however, detection performance deteriorated significantly. YOLOv5s reached the confidence threshold at only 36.45 ft, while YOLOv8s failed to achieve the threshold altogether. These results indicate that fog had a severe negative impact on truck detection performance for both algorithms.

Overall, compared with the baseline condition, reducing the FOV from 90° to 45° increased the distance at which the confidence threshold was achieved for both pedestrian and truck detection under sunny conditions. However, adverse weather conditions reduced detection performance, with the most significant degradation observed under foggy conditions. Under the baseline configuration, YOLOv5s demonstrated better performance for pedestrian detection, whereas YOLOv8s achieved superior truck detection performance under clear and rainy conditions with the 45° FOV configuration. YOLOv8 generally improves localization, feature extraction, and robustness but the smaller versions (“s” models) used in this study may not be consistently better than depending on object class, image resolution, and simulation rendering.

It should be noted that the machine vision models were trained using data collected under sunny conditions only. Therefore, improved detection performance under adverse weather conditions may be achieved through additional training and validation using datasets representing rain, fog, and other challenging environmental conditions.

The results indicate that the distance to detect trucks is about 310 feet and to detect a pedestrian is about 225 feet in sunny condition. Previous real-world testing of high-resolution forward-facing onboard cameras in daylight conditions indicates that the detection distance of a pedestrian is 100 ft to 164 ft and for a bigger object like car is 100 ft to 328 ft (Kumar et al., 2020). This indicates that the detection distances obtained in this study are reasonable. The increase in the detection distance with the reduction in focal length is also realistic. This is because a narrower FOV increases pixel density and enlarges object representation in the image.

Regarding the deterioration in detection performance under adverse conditions. The results show moderate degradations under rain (225 ft to 172 ft for pedestrian detection and 310 ft to 238 ft for truck detection). The results show also severe degradation with fog (225 ft to 83 ft for pedestrian detection and 310 ft to 36 ft for truck detection). Although the results are consistent with real-world testing (Bijelic et al., 2020; Sakaridis et al., 2021) that fog is more destructive to vision systems than rain, the reduction in the detection with fog seems to be more than what is expected. This is possibly dependent on the utilized fog density and that CARLA fog settings produced stronger visibility degradation than moderate real-world fog conditions.

Overall, the results support the following conclusions:

- Narrower FOV cameras substantially improve object detection performance.
- Fog produces significantly larger degradation than rain.
- Large objects (trucks) are detectable at longer ranges than pedestrians.
- YOLOv8s provides improved robustness for larger vehicle detection under adverse conditions.
- CARLA-generated detection ranges are generally consistent with trends observed in real-world automotive perception studies.

4.1.2. Precision Analysis

As described in Section 2, Precision is a parameter that measures the proportion of correct detection instances among all reported detections, indicating how often the model's detections are accurate. **Error! Reference source not found.** presents the precision results for both detected object classes (pedestrian and truck) under all test scenarios.

For the pedestrian class, the test results indicate that precision varied depending on weather conditions and FOV. In general, both models showed lower precision in sunny wide-view settings and improved precision under rainy or foggy scenarios, likely because fewer distant low-quality detections were produced. YOLOv8s achieved the highest pedestrian precision under 45° Rain (0.857), while YOLOv5s achieved strong results under 45° Fog (0.84).

For the truck class, both models achieved 100% precision in all scenarios, meaning every truck detection was correct with no false positives. This indicates that trucks were easier to identify because of their larger size and clearer visual features.

Overall, truck detection was consistently more reliable than pedestrian detection, while pedestrian precision was influenced by visibility conditions and camera FOV.

Table 4-2 Comparison of Model Precision under Different Test Scenarios

Scenario	Pedestrian			Truck		
	True Positive	False Positive	Precision	True Positive	False Positive	Precision
Yolov5s Fov 90 Sunny	2189	596	0.79	100	0	1.00
Yolov5s Fov 45 Sunny	3519	1321	0.73	100	0	1.00
Yolov5s Fov 45 Rain	2732	552	0.83	100	0	1.00
Yolov5s Fov 45 Fog	1532	289	0.84	100	0	1.00
Yolov8s Fov 90 Sunny	1640	766	0.68	100	0	1.00
Yolov8s Fov 45 Sunny	3017	1228	0.71	100	0	1.00
Yolov8s Fov 45 Rain	2984	497	0.86	100	0	1.00
Yolov8s Fov 45 Fog	1601	649	0.71	100	0	1.00

4.1.3. Inference Time Analysis

As described earlier, inference time is defined as the computational time required by the detection model to process one frame and produce an output. **Error! Reference source not found.** presents the inference time performance of YOLOv8s and YOLOv5s models under different environmental and camera configurations.

YOLOv8s consistently demonstrated faster average inference times than YOLOv5s across most scenarios. Under sunny conditions, YOLOv8s recorded average inference times of 10.69 ms for FOV 90° and 10.57 ms for FOV 45°, whereas YOLOv5s required 12.04 ms and 12.33 ms, respectively. These results indicate that YOLOv8s provides better computational efficiency under clear-weather conditions. It should be noted that the Inference Time is a function of the computer used in processing the information. The computer used in the testing of this study is equipped with an Intel Core i7-10700K processor, 32 GB RAM, and an NVIDIA GeForce RTX 3070 GPU.
Under rainy conditions, YOLOv8s maintained lower average inference times, with 10.99 ms for pedestrian detection and 11.25 ms for truck detection, compared with 12.44 ms and 12.38 ms for YOLOv5s. This suggests that YOLOv8s remains computationally efficient under moderate visibility degradation.

Under foggy conditions, the inference times increased for both models, likely because degraded image quality required more complex feature extraction and processing. YOLOv5s increased to 13.60 ms for pedestrian detection and 13.75 ms for truck detection, while YOLOv8s increased to 12.77 ms and 12.48 ms, respectively.

Overall, YOLOv8s demonstrated better computational efficiency across most scenarios for both pedestrian and truck detection. Rain and Fog increased the inference times for both models, while YOLOv8s generally maintained lower average inference times and more stable processing performance than YOLOv5s.

Table 4-3 Comparison of Inference Time (ms) under Different Test Scenarios

Scenario	Pedestrian **Detection**				**Truck Detection**			
	Average	**Standard Deviation**	**Minimum**	**Maximum**	**Average**	**std**	**min**	**max**
Yolov5s FOV 90 Sunny	12.04	2.03	9.14	22.85	11.98	1.93	9.14	22.85
Yolov5s FOV 45 Sunny	12.33	1.92	9.51	22.23	12.33	1.96	9.51	22.23
Yolov5s FOV 45 Rain	12.44	2.11	9.42	23.41	12.38	2.13	9.42	23.41
Yolov5s FOV 45 Fog	13.60	2.18	9.49	18.48	13.75	2.18	9.60	18.38
Yolov8s FOV 90 Sunny	10.69	1.21	9.07	19.54	10.93	1.29	9.08	19.65
Yolov8s FOV 45 Sunny	10.57	1.32	8.81	20.87	10.79	1.21	8.81	20.87
Yolov8s FOV 45 Rain	10.99	1.05	8.87	23.08	11.25	1.06	8.72	23.08
Yolov8s FOV 45 Fog	12.77	2.34	8.52	20.25	12.48	2.51	9.16	15.52

4.2 Subject Vehicle Performance during Lane Change

This section presents the results of the evaluation of the SV during lane-changing maneuvers performed upstream of the work zone, where the SV switched from the blocked lane to the adjacent target lane. The analysis examines the effects of different merging strategies on lane-changing performance under two traffic demand levels: a relatively low demand of 1,000 vehicles/hour/lane and a high-demand condition near capacity at 2,200 vehicles/hour/lane.

Table 4-4 summarizes the performance of the SV under the two demand conditions for four merging scenarios. The first scenario assumes no cooperation between the lane-changing AV and vehicles in the target lane, which are assumed to be human driven (HV-OVs in the test plan). This condition represents low market penetration of CAVs, where V2V communication is unavailable and the AV relies solely on the autonomous lane-changing behavior implemented in the OpenCDA platform. This scenario serves as the baseline for evaluating the impacts of CDA control algorithms.

Table 4-4 Impacts of Merging Strategies on Subject Vehicle Performance

Measure	**Statistic**	**No cooperation**		**Cut-in joining**		**Back joining**		**Front joining**	
		1,000 vphpl	**2,200 vphpl**	**1,000 vphpl**	**2,200 vphpl**	**1,000 vphpl**	**2,200 vphpl**	**1,000 vphpl**	**2,200 vphpl**
Lane-change completion time (s)	Mean	2.83	4.67	2.66	3.14	1.40	5.05	2.50	3.92
	Std	0.54	1.74	0.07	0.75	0.00	0.02	0.00	0.57
	Min	2.10	1.15	2.60	2.80	1.40	5.00	2.50	2.85
	Max	3.50	7.35	2.80	5.25	1.40	5.05	2.50	4.20
Lead distance gap (ft)/ lead time gap (sec)	Mean	121.55/2.25	52.99/18.29	31.72/0.50	16.86/0.66	17.75/0.31	47.70/1.78	356.44/5.53	242.89/8.92
	Std	97.29/1.79	12.22/47.47	0.28/0.02	0.51/0.03	0.20/0.01	0.21/0.01	70.12/0.96	63.58/2.22
	Min	42.03/0.78	41.40/1.52	31.37/0.49	15.62/0.60	17.49/0.30	47.11/1.75	274.84/4.35	135.70/5.05
	Max	380.84/7.01	71.16/152.85	32.19/0.54	17.22/0.67	17.98/0.34	47.77/1.78	465.58/7.17	341.11/12.39
Lead distance gap (ft)/ lead time gap (sec	Mean	211.26/3.65	93.30/3.58	45.32/0.85	26.03/1.13	159.04/2.44	245.45/9.01	58.79/0.93	57.12/3.02
	Std	148.75/2.93	84.07/3.60	0.69/0.01	3.68/0.17	39.90/0.77	22.44/1.74	0.20/0.01	60.00/2.89
	Min	47.41/0.82	16.27/0.53	44.55/0.84	15.68/0.66	126.21/1.83	207.09/7.77	58.73/0.92	28.54/1.69
	Max	467.22/9.79	290.39/12.13	46.69/0.87	28.58/1.25	265.68/4.51	281.10/13.35	59.35/0.97	172.47/9.86
SV speed at end (mph)	Mean	36.98	18.12	37.57	17.82	29.45	18.28	43.84	15.24
	Std	0.07	0.16	0.93	0.33	0.25	0.23	3.32	0.62
	Min	36.91	17.90	36.31	17.16	29.26	18.05	35.57	14.65
	Max	37.09	18.34	38.88	18.46	30.00	18.70	46.19	16.46
Lead vehicle speed at end (mph)	Mean	45.31	20.74	43.45	20.12	42.73	16.38	47.76	21.64
	Std	2.56	1.01	2.17	0.90	3.22	1.40	1.13	0.96
	Min	42.41	18.50	38.92	18.23	33.82	12.42	46.19	20.16
	Max	51.34	21.81	45.30	21.39	44.11	17.09	49.79	23.18
Lag vehicle speed at end (mph)	Mean	38.74	14.34	39.12	18.39	39.49	12.67	45.13	16.35
	Std	3.35	3.47	0.76	1.27	0.93	0.32	2.02	0.58
	Min	32.53	9.87	37.78	15.70	37.54	12.46	41.38	15.14

Measure	Statistic	No cooperation		Cut-in joining		Back joining		Front joining	
		1,000 vphpl	**2,200 vphpl**	**1,000 vphpl**	**2,200 vphpl**	**1,000 vphpl**	**2,200 vphpl**	**1,000 vphpl**	**2,200 vphpl**
	Max	43.29	18.79	40.49	19.06	40.49	13.31	47.47	17.05
TTC to lead (s)	Mean	NA	NA	NA	NA	NA	1.20	NA	NA
	Std	NA	NA	NA	NA	NA	0.12	NA	NA
	Min	NA	NA	NA	NA	NA	0.88	NA	NA
	Max	NA	NA	NA	NA	NA	1.27	NA	NA
TTC to lag (s)	Mean	3.22	5.74	0.90	1.13	2.52	NA	0.89	2.15
	Std	2.11	NA	0.03	0.02	0.82	NA	0.03	3.58
	Min	0.60	5.74	0.84	1.09	1.86	NA	0.87	0.89
	Max	6.16	5.74	0.94	1.16	4.71	NA	0.95	11.69
Mean acceleration during LC (ft/s^2)	Mean	0.01	0.88	-2.96	0.20	-10.01	0.05	-0.06	-1.17
	Std	0.08	1.75	0.73	0.36	1.33	0.07	0.08	0.27
	Min	-0.07	-0.19	-4.27	-0.65	-10.64	-0.04	-0.17	-1.41
	Max	0.14	4.90	-1.98	0.44	-6.32	0.17	0.00	-0.57
Mean jerk during LC (ft/s^3)	Mean	140.27	129.45	271.60	130.10	305.86	55.57	101.36	100.46
	Std	34.31	113.41	85.69	22.54	95.48	1.17	110.52	26.90
	Min	99.65	75.80	142.70	72.69	37.40	54.66	0.00	73.80
	Max	185.74	449.28	378.03	158.40	375.70	58.01	231.43	159.22

Note: NA indicates undefined or not applicable.

The remaining three scenarios involve the use of CDA control algorithms for cooperative merging supported through V2V communication between the SV and a platoon of cooperative automated vehicles (CDA-OVs in the test plan) traveling in the adjacent lane. In these scenarios, the SV joins the platoon either in the middle of the platoon (cut-in joining), at the rear of the platoon (back joining), or at the front of the platoon (front joining).

The first performance measure used in the comparison was the time required to complete the lane-change maneuver. Under the 1,000 vehicles/hour/lane demand condition, only the back-joining strategy produced a meaningful reduction in average lane-change completion time, reducing it to 1.40 seconds compared with 2.83 seconds under the no-cooperation condition. However, it should be noted that this could be due to the position of the merging vehicle in the blocked lane relative to the platoon, which is closer to the back of the platoon than the front of the platoon.

Under the 2,200 vehicles/hour/lane demand condition, cut-in joining resulted in the shortest average lane-change completion time at 3.14 seconds, compared with 4.67 seconds for the no-cooperation condition. These findings indicate that higher traffic demands generally made lane changing more difficult and that the completion of the lane change is easier with cut-in merging under high demand conditions as cooperative vehicles within the platoon coordinated to open a gap that facilitated cut-in joining.

The second measure examined was the accepted lead gap and lag gap at the initiation of the lane change. The lead gap represents the spacing between the SV and the lead vehicle in the target lane, while the lag gap represents the spacing between the SV and the following vehicle in the target lane. Under the 1,000 vehicles/hour/lane condition and with no cooperation, the mean lag distance gap and mean lag speed gap were 211.26 ft and 3.65 s, while corresponding values for the lead gap were 121.55 ft and 2.25 s. These gaps are higher than the gaps left to vehicle in platoons during cooperative lane change, reflecting the relatively conservative behavior of the OpenCDA lane-changing algorithm when interacting with human-driven traffic.

In contrast, the cooperative merging strategies accepted substantially smaller gaps within the platoon. For back joining, the mean lag (to human driven) and lead gaps (to last vehicle in platoon) were 159.04 ft corresponding to 2.44 s and 17.75 ft corresponding to 0.31 s, respectively. For cut-in joining, the gaps were 45.32 ft corresponding to 0.85 s and 31.72 ft corresponding to 0.50 s, while front joining resulted in lag gap of 58.79 ft (corresponding to 0.93 s) to first vehicle in platoon and lead gap of 356.44 ft (corresponding 5.53 s) (to human driven vehicle), respectively. In addition, the standard deviations of the accepted gaps within the platoon were relatively small, indicating highly consistent merging behavior. These results suggest that although the AV maintained relatively conservative gaps when merging with human-driven vehicles, it merged into cooperative platoons using significantly smaller spatial and temporal gaps.

Similar trends were observed under the 2,200 vehicles/hour/lane condition. With no cooperation, the mean lag and lead gaps were 93.30 ft (3.58 s) and 52.99 ft (18.29 s), respectively, indicating substantially smaller accepted distance gaps than those observed under low demand but higher time gaps due to the low speed. For cooperative merging, the lag/lead gaps for back joining, cut-in joining, and front joining were 245.45 ft (9.01 s)/47.70 ft (1.78 s), 26.03 ft (1.13 s)/16.86 ft (0.66 s), and 57.12 ft (3.02)/242.89 ft (8.92 s), respectively. These findings further confirm that the cooperative algorithms allowed the SV to merge into platoons using very short gaps and low spatial and temporal margins.

The relative speeds between the SV and the lead and lag vehicles in the target lane after finishing the lane changing maneuver provide additional insight into the observed merging behavior. At 1,000 vehicles/hour/lane, the SV speed at the end of the lane change averaged 36.98 mph, compared with 38.74 mph for the lag vehicle and 45.31 mph for the lead vehicle. This resulted in a TTC of approximately 3.22 seconds with respect to the lag vehicle. Under the 2,200 vehicles/hour/lane condition, the corresponding speeds were 18.12 mph for the SV, 14.34 mph for the lag vehicle, and 20.74 mph for the lead vehicle. It should be noted that when the lead vehicle speed is higher than the lag/following vehicle speed, the TTC is generally considered undefined or not applicable (N/A).

For cut-in joining under the 1,000 vehicles/hour/lane condition, the SV speed was lower than the lag vehicle speed (37.57 mph versus 39.12 mph). At the same time, the SV speed was lower than the lead vehicle speed (37.57 mph versus 43.45 mph). Although this cooperative behavior enabled rapid insertion into the platoon, it resulted in a TTC of only 0.90 seconds relative to the lag vehicle, accompanied by a deceleration of 2.96 ft/s² and a jerk of 271.60 ft/s³. Under the 2,200 vehicles/hour/lane condition, the SV speed was 17.82 mph compared with 18.39 mph for the lag vehicle and 20.12 mph for the lead vehicle. In this case, the smaller relative speed differences reduced the likelihood of immediate collision risk despite the shorter accepted gaps.

For back joining under the 1,000 vehicles/hour/lane condition, the SV speed was 29.45 mph compared with 42.73 mph for the lead vehicle, resulting in a TTC of 2.52 seconds relative to the lag vehicle, along with a deceleration of 10.01 ft/s² and a jerk of 305.86 ft/s³. Under the 2,200 vehicles/hour/lane condition, the corresponding speeds were 18.28 mph for the SV and 16.38 mph for the lead vehicle, resulting in a TTC of approximately 1.20 seconds.

For front joining, the SV speed relative to the lag vehicle was 43.84 mph versus 45.13 mph under the 1,000 vehicles/hour/lane condition and 15.24 mph versus 16.35 mph under the 2,200 vehicles/hour/lane condition, resulting in TTC values to the lag vehicle of approximately 0.89 seconds and 2.15 seconds.

Overall, these results indicate that the tested cooperative algorithms adjusted the SV speed relative to platoon vehicles such that the SV speed generally remained equal to or higher than the lag vehicle speed and equal to or lower than the lead vehicle speed. While this behavior facilitated rapid insertion into the platoon, the SV frequently merged with very low TTC values relative to nearby platoon vehicles. In particular, under low demand, cut-in and back joining produced very small TTC values relative to the lead vehicle, while front joining produced small TTC values relative to the lag vehicle. These results suggest that although the cooperative strategies improved merging efficiency, they may also introduce potential safety concerns due to the extremely small temporal gaps accepted during platoon joining maneuvers. This is particularly true under low demand conditions that can result in breaking to increase the TTC and larger speed differentials between the lead and lag vehicles.

In OpenCDA, the lane-changing behavior of the CDA vehicle is controlled by a rule-based algorithm called the Behavior Agent. At each simulation step, the agent first updates the subject vehicle's position, speed, and surrounding vehicles, then generates a future path. During the simulation, if the SV needs to change lanes due to the planned route or the presence of a slower/blocking vehicle ahead, the agent evaluates whether the lane change is allowed. This evaluation considers several conditions, including road curvature, collision risk, and whether the vehicle is already performing another maneuver. For safety checking, the algorithm generates a short path toward the target lane and checks this path against nearby vehicles. If no potential collision is detected, the lane change is allowed. Otherwise, the lane change is rejected, and the vehicle may continue in the current lane, slow down, or follow the vehicle ahead.

The main limitation of this lane-changing algorithm is that it is rule-based and depends heavily on predefined thresholds, such as distance, angle, speed, curvature, and collision-checking conditions. Therefore, the vehicle does not optimize the lane-change decision based on traffic efficiency or long-term platoon stability. It only checks whether the maneuver is currently allowed or unsafe. The algorithm also has limited adaptability in complex traffic conditions because it does not explicitly predict surrounding vehicles' future behavior beyond the short collision-checking horizon.

4.3 Surrounding Vehicle Performance

Next, this study assessed the impact of the lane-change maneuver on the performance and stability of the surrounding vehicles. Primary measures used in this assessment of traffic string stability is the standard deviation of speeds across vehicles (SDt), standard deviation of speed over time for individual vehicles (SDv), and the oscillation percentage. These measures reflect the degree of platoon stability and synchronization following the merge maneuver. Lower values indicate that disturbances are effectively damped and that the platoon remains stable, whereas higher values indicate stronger disturbance propagation and reduced string stability.

The results in Table 4-5 show that both upstream and downstream oscillations increased substantially under the 2,200 vehicles/hour/lane demand condition compared with the 1,000 vehicles/hour/lane condition across all merging strategies. This indicates that congested traffic conditions significantly increased the propagation of speed disturbances through the platoon. The increase in oscillation percentages under congested conditions was accompanied by corresponding increases in the standard deviation of vehicle speeds, confirming that congestion reduced the ability of the platoon to absorb merge disturbances smoothly.

Among the evaluated strategies, Table 4-5 indicates that cut-in joining produced the lowest upstream speed variability under the 2,200 vehicles/hour/lane condition (the congested conditions). The mean upstream SDv was 0.78 ft/s for cut-in joining, compared with 1.61 ft/s for no cooperation, 1.33 ft/s for back joining, and 1.90 ft/s for front joining. The mean upstream SDt was 0.81 ft/s for cut-in joining, compared with 1.35 ft/s for no cooperation, 1.08 ft/s for back joining, and 1.32 ft/s for front joining. Similarly, cut-in joining produced the lowest upstream oscillation percentage under congested conditions at 44.33%, compared with 55.50% for no cooperation, 68.00% for back joining, and 78.21% for front joining. In addition, cut-in joining resulted in relatively low lag-vehicle deceleration and the shortest lane-change completion time under congested traffic conditions. These findings indicate that cooperative cut-in joining was the most string-stable strategy under high traffic demand conditions.

However, the front and back joining did not have similar positive impacts on improving string stability compared to changing lane with no cooperation. For example, front joining at 2,200 vehicles/hour/lane resulted in upstream oscillation percentages of 78.21% and 76.67%, respectively, along with the highest upstream speed variability (SDv 1.90 ft/s and SDt of 1.32). These results indicate that the disturbances introduced at the front of the platoon due to the lane changing vehicle propagated through the vehicle string. Back joining resulted in 68% oscillation, SDv of 1.33 ft/s, and SDv of 1.35 ft/sec of the upstream string.

During uncongested conditions, the cooperative scenarios, particularly the back joining and cut-in joining, caused significant increases in the oscillation. This is most likely due to merging at relatively high speed with low TTC, resulting in braking and speed differential. In particular, severe braking was observed during back joining under the low-demand condition. At 1,000 vehicles/hour/lane, back joining produced a mean maximum lag-vehicle deceleration of −16.13 ft/s^2, compared with −3.21 ft/s^2 for no cooperation, −5.99 ft/s^2 for cut-in joining, and −0.85 ft/s^2 for front joining. Although traffic demand was relatively low, higher free-flow speeds and larger speed differentials increased aggressive speed adjustments resulting in substantial local breaking despite the lower traffic density.

Table 4-5 Impacts of Merging Strategies on Other Vehicle Performance

Measure	Statistic	No cooperation		Cut-in joining		Back joining		Front joining	
		1,000 vphpl	**2,200 vphpl**	**1,000 vphpl**	**2,200 vphpl**	**1,000 vphpl**	**2,200 vphpl**	**1,000 vphpl**	**2,200 vphpl**
SDt upstream (ft/s)	Mean	2.66	1.35	1.06	0.81	3.47	1.08	2.01	1.32
	Std	1.04	1.24	0.28	0.30	1.52	0.16	0.99	0.34
	Min	1.49	0.34	0.74	0.49	2.04	0.81	0.87	0.88
	Max	4.34	4.38	1.59	1.52	5.56	1.30	3.81	2.06
SDv upstream (ft/s)	Mean	0.66	1.61	0.72	0.78	1.61	1.33	0.45	1.90
	Std	0.78	1.52	0.09	0.36	0.57	0.11	0.14	0.49
	Min	0.00	0.20	0.59	0.30	0.54	1.22	0.22	0.67
	Max	2.16	4.36	0.82	1.40	2.68	1.52	0.71	2.36
Oscillation upstream (%)	Mean	5.33	55.50	53.33	44.33	33.33	68.00	12.92	78.21
	Std	11.68	14.23	10.54	19.18	13.61	16.87	14.06	10.34
	Min	0.00	40.00	33.33	20.00	0.00	40.00	0.00	62.50
	Max	33.33	80.00	66.67	80.00	50.00	100.00	37.50	100.00
Lag vehicle maximum deceleration (ft/s^2)	Mean	-3.21	-8.77	-5.99	-1.01	-16.13	-2.60	-0.85	-8.57
	Std	4.41	8.74	4.25	1.07	0.89	0.72	0.63	6.60
	Min	-13.94	-29.53	-17.06	-2.64	-17.88	-4.04	-1.77	-26.02
	Max	0.00	0.00	-1.31	0.00	-14.70	-1.71	0.00	-2.53

5. Conclusions

This study investigated the use of co-simulation to evaluate CDA applications within a work zone environment. The examined use case focused on the merging maneuvers of a single CDA-equipped vehicle into either a CDA platoon or a traffic stream of human-driven vehicles near a work zone with a one-lane blockage. The findings demonstrate that co-simulation can serve as an effective component of AV and CDA testing, particularly in complex and challenging environments such as work zones. Overall, the results indicate that co-simulation is a practical and flexible tool for evaluating CDA operations in realistic and complex traffic scenarios. The study further shows that cooperative lane-changing behavior near work zones can be systematically assessed within a controlled simulation environment, and that the resulting performance measures can help identify limitations and inform potential improvements to existing automated and cooperative driving logic.

The test plan and procedures were developed in accordance with IEEE standards. Although tailored to the selected case study, the test plan is intended to serve as a reference framework for evaluating other automated and cooperative vehicle operations within co-simulation and digital twin environments.

The results from evaluating the co-simulation platform's ability to represent and detect work zone features, such as trucks and pedestrians, indicate reasonable agreement between the video image–based detection distances obtained in simulation and those reported in previous real-world studies. The study also confirms several established observations from the literature, including that narrower camera FOV can significantly improve object detection performance; fog conditions cause substantially greater degradation in detection accuracy than rain; and larger objects such as trucks are detectable at longer ranges than pedestrians. In addition, the results indicate that YOLOv8s demonstrates improved robustness for detecting larger vehicles under adverse conditions compared to YOLOv5s.

This study evaluated the ability of co-simulation to assess the performance of CDA lane-changing strategies upstream of a work zone using the OpenCDA co-simulation platform under two traffic demand levels: a low-demand condition of 1,000 vehicles/hour/lane and a high-demand condition near capacity at 2,200 vehicles/hour/lane. Four merging scenarios were examined, including a non-cooperative baseline condition and three cooperative platoon joining strategies: cut-in joining, back joining, and front joining. The results showed that both traffic demand and merging strategy affected SV performance and the impact of the merging maneuvers on the surrounding traffic behavior.

The results demonstrated that the effectiveness of the merging strategy, as implemented in OpenCDA depended strongly on traffic demand conditions. In general, the cooperative merging strategies enabled the SV to merge into platoons using substantially smaller spatial and temporal gaps than those accepted under the non-cooperative condition. While the default OpenCDA lane-changing behavior produced relatively conservative accepted gaps and TTC values when interacting with human-driven traffic, the cooperative algorithms consistently generated very short accepted gaps and low TTC values during platoon insertion maneuvers.

In several cases, particularly under low-demand traffic conditions, the cut-in and, more notably, the back-joining strategies produced TTC values below one second relative to nearby platoon vehicles. These short temporal gaps resulted in braking maneuvers and increased speed differentials that may adversely affect safety. The results indicate that, under the tested CDA control algorithm, lower traffic demand did not necessarily lead to smoother or safer platoon insertion maneuvers. Instead, the acceptance of very short gaps at relatively high speeds contributed to abrupt braking and larger speed variations among vehicles. Although the cooperative merging strategies improved merging efficiency, the extremely short temporal margins accepted by the control logic may raise concerns regarding safety, ride comfort, and system robustness, particularly under communication delays, sensing uncertainty, or unexpected vehicle behavior.

The results further demonstrated that lane-changing maneuvers can significantly affect platoon stability and disturbance propagation. Congested traffic conditions increased both upstream oscillations across all strategies, indicating that higher traffic demand reduced the ability of the platoon to absorb disturbances smoothly. The increase in oscillatory behavior was accompanied by increased speed variability, confirming the degradation of string stability under high traffic demand.

Among the evaluated strategies, cooperative cut-in joining produced the most stable behavior under congested conditions. This strategy generated the lowest upstream speed variability, the lowest upstream oscillation percentage, relatively low lag-vehicle deceleration, and the shortest lane-change completion time. These findings suggest that coordinated gap creation within the platoon effectively distributed merge disturbances and reduced abrupt spacing corrections. In contrast, the non-cooperative condition resulted in stronger disturbance propagation and higher oscillation levels. Back joining and front joining did not have similar positive effects on stability under congested conditions, and both produced higher oscillation percentages compared to no cooperation. Front joining produced the highest instability levels under congested traffic conditions.

Overall, the study demonstrates that cooperative lane-changing strategies can substantially improve merging efficiency relative to non-cooperative automated driving behavior. However, the results also show that aggressive cooperative platoon insertion using extremely small temporal gaps may introduce safety concerns and string instability, particularly under congested traffic conditions or when large speed differentials exist between the merging vehicle and platoon vehicles. Therefore, updates to the tested cooperative lane-changing algorithm and its associated control parameters are recommended to reduce the acceptance of excessively short gaps that result in critically low TTC values. Cooperative merging algorithms should incorporate explicit minimum TTC and time-headway constraints to the lead and lag vehicles during platoon insertion maneuvers.

The analysis also identified several limitations of the evaluated control framework. The planning layer currently makes lane-changing decisions primarily based on gap availability and vehicle speed, without explicitly considering acceleration profiles or predicting future vehicle behavior. In addition, the tested algorithm employs a proportional–integral–derivative (PID) controller in the actuation layer, which is less sophisticated than advanced control approaches such as Model Predictive Control (MPC) that are better suited for handling complex and nonlinear vehicle dynamics. Because the PID controller is primarily reactive and does not optimize future control actions, it can result in inefficient or abrupt vehicle responses.

The investigated merging strategy is governed by a finite-state machine and heuristic decision rules that rely mainly on simple distance-based criteria, without accounting for dynamic traffic factors such as relative speed, acceleration behavior, or anticipated traffic evolution. Furthermore, the system uses predetermined merging gap thresholds and limited cooperative behavior, where control adjustments are primarily performed by the rear vehicle, without fully considering the broader interactions among surrounding traffic and platoon vehicles.

Future work should focus on enhancing both the planning and control logic of the automated driving framework, expanding cooperative coordination among platoon vehicles, and evaluating the framework under a wider range of traffic and roadway conditions. Cooperative lane-changing controllers could incorporate stability-oriented objectives in addition to merge-efficiency objectives. The adoption of more advanced control methods, together with the integration of string stability constraints, acceleration smoothing, and jerk minimization into the control logic, could help reduce disturbance propagation throughout the platoon and improve ride comfort and safety.

The findings of this study indicate the need for improving the investigated lane-changing logic, which is the default logic implemented in OpenCDA. This improvement may include simultaneously considering both lead-vehicle and lag-vehicle gaps and their combined effects when changing lanes, modifying platoon behavior by allowing the lead vehicle to accelerate in addition to reducing the speed of the lag vehicle, and implementing infrastructure-based adaptive parameter settings to improve lane-changing performance under varying traffic conditions.

Infrastructure-supported merging maneuvers have the potential to significantly improve operational performance and safety. For example, infrastructure-based adaptive merging strategies could be implemented according to prevailing traffic demand conditions, where the infrastructure provides guidance on the most appropriate merging strategy (e.g., cut-in, back joining, or front joining) as well as associated merging parameters. The infrastructure could also provide additional operational guidance, including designated lane usage for CDA platoons, recommended merge locations, dynamic updates to inter-platoon and intra-platoon gaps at specified distances upstream of the work zone, ODD takeover points for drivers, recommended CDA vehicle speeds, platoon size limits, and other cooperative control parameters.

Future work may extend this research through the development of a digital twin framework incorporating VIL, HIL, and field testing to further evaluate cooperative driving automation strategies for roadway approaches to work zones with lane blockages.

6. References

Benjumea, A., Teeti, I., Cuzzolin, F., & Bradley, A. (2021). YOLO-Z: Improving Small Object Detection in YOLOv5 for Autonomous Vehicles. *arXiv preprint*. https://arxiv.org/abs/2112.11798

Bi, X., Weng, C., Tong, P., Li, D., Yang, X., & Zhao, G. (2022). *Virtual Verification of Millimeter-Wave Radar Function of an Autonomous Vehicle under Weather Interference* (SAE Technical Paper, Issue.

Bijelic, M., Gruber, T., Mannan, F., Kraus, F., Ritter, W., Dietmayer, K., & Heide, F. (2020). *Seeing Through Fog Without Seeing Fog: Deep Multimodal Sensor Fusion in Unseen Adverse Weather*. https://doi.org/10.1109/CVPR42600.2020.01170

Cui, D., Shen, Y., Yang, H., Huang, Z., Rush, K., Huang, P., & Bujanovic, P. (2023). Extensible Co-Simulation Framework for Supporting Cooperative Driving Automation Research. *Transportation Research Record: Journal of the Transportation Research Board*, *2677*(3), 1067-1079. https://doi.org/10.1177/03611981221121263

Dazlee, N. M. A. A., Khalil, S. A., Abdul-Rahman, S., & Mutalib, S. (2022). Object Detection for Autonomous Vehicles with Sensor-Based Technology Using YOLO. *International Journal of Intelligent Systems and Applications in Engineering*, *10*(1), 129-134.

Dosovitskiy, A., Ros, G., Codevilla, F., Lopez, A., & Koltun, V. (2017). CARLA: An Open Urban Driving Simulator. Conference on Robot Learning,

Epic, G. (2024/09). *Unreal Engine*. https://www.unrealengine.com/

Federal Highway Administration. *carma-platform*. https://github.com/usdot-fhwa-stol/carma-platform

Federal Highway Administration. (2024). *An Open-Source Cosimulation Tool to Support Cooperative Driving Automation (CDA) Research*. https://doi.org/10.21949/1521619

Hsu, W. Y., & Lin, W. Y. (2021). Adaptive Fusion of Multi-Scale YOLO for Pedestrian Detection. *IEEE Access*, *9*, 110063-110073.

Ieee. (2008). IEEE Standard for Software and System Test Documentation. *IEEE Std 829-2008*, 1-150.

Jocher, G. (2020, 2023/02/30). *YOLOv5 by Ultralytics*. https://github.com/ultralytics/yolov5

Jocher, G., Chaurasia, A., & Qiu, J. (2023, 2023/02/30). *YOLO by Ultralytics*. https://github.com/ultralytics/ultralytics

Kim, T., Jeon, H., & Lim, Y. (2023). Challenges of YOLO Series for Object Detection in Extremely Heavy Rain: CARLA Simulator Based Synthetic Evaluation Dataset. *ArXiv*. https://doi.org/10.48550/arXiv.2312.07976

Kumar, G. A., Lee, J. H., Hwang, J., Park, J., Youn, S. H., & Kwon, S. (2020). LiDAR and Camera Fusion Approach for Object Distance Estimation in Self-Driving Vehicles. *Symmetry*, *12*(2), 324. https://www.mdpi.com/2073-8994/12/2/324

Lab, U. M. (2024, 2024/09). *OpenCDA Documentation*. https://opencda-documentation.readthedocs.io/en/latest/index.html

Lan, W., Dang, J., Wang, Y., & Wang, S. (2018). Pedestrian Detection Based on YOLO Network Model. 2018 IEEE International Conference on Mechatronics and Automation (ICMA),

Li, Q., Ding, X., Wang, X., Chen, L., Son, J., & Song, J. Y. (2021). Detection and Identification of Moving Objects at Busy Traffic Road Based on YOLO v4. *The Journal of the Institute of Internet, Broadcasting and Communication*, *21*(1), 141-148.

Liang, S., Wu, H., Zhen, L., Hua, Q., Garg, S., Kaddoum, G., Hassan, M. M., & Yu, K. (2022). Edge YOLO: Real-Time Intelligent Object Detection System Based on Edge-Cloud Cooperation in Autonomous Vehicles. *IEEE Transactions on Intelligent Transportation Systems*, *23*(12), 25345-25360.

Lin, T. Y., Maire, M., Belongie, S., Bourdev, L., Girshick, R., Hays, J., Perona, P., Ramanan, D., Zitnick, C. L., & Dollár, P. (2015). Microsoft COCO: Common Objects in Context.

Lopez, P. A., Behrisch, M., Bieker-Walz, L., Erdmann, J., Flötteröd, Y. P., Hilbrich, R., Lücken, L., Rummel, J., Wagner, P., & Wießner, E. (2018). Microscopic Traffic Simulation Using SUMO. 2018 21st International Conference on Intelligent Transportation Systems (ITSC),

Sakaridis, C., Dai, D., & Gool, L. (2021). *ACDC: The Adverse Conditions Dataset with Correspondences for Semantic Driving Scene Understanding*. https://doi.org/10.1109/ICCV48922.2021.01059

Stevens, A., & Hopkin, J. (2012). *Benefits and deployment opportunities for vehicle/roadside cooperative ITS*. https://doi.org/10.1049/cp.2012.1535

Terven, J., & Cordova-Esparza, D. (2023). A Comprehensive Review of YOLO Architectures in Computer Vision: From YOLOv1 to YOLOv8 and YOLO-NAS. *Machine Learning and Knowledge Extraction*, *5*(4), 1680-1716. https://www.mdpi.com/2504-4990/5/4/83

Xu, R., Guo, Y., Han, X., Xia, X., Xiang, H., & Ma, J. (2021). Opencda: an open cooperative driving automation framework integrated with co-simulation. 2021 IEEE International Intelligent Transportation Systems Conference (ITSC),

Yaml. (2023, 2023/05/25). *YAML*. https://yaml.org

Zhang, Y., Carballo, A., Yang, H., & Takeda, K. (2021). Autonomous Driving in Adverse Weather Conditions: A Survey. *arXiv preprint*. https://doi.org/10.48550/arXiv.2112.08936